High frequency visual stimulation primes gamma oscillations for visually-evoked phase reset and enhances spatial acuity

Crystal L. Lantz[1], and Elizabeth M. Quinlan[1]*

[1] Department of Biology and Neuroscience and Cognitive Sciences Program; University of Maryland; College Park, MD, 20742; USA

* Corresponding Author, equinlan@umd.edu

Abstract

The temporal frequency of synaptic activation is a decisive factor in the regulation of perceptual detection thresholds following high or low frequency sensory stimulation. However, surprisingly little is known about the neuronal and circuit level responses to distinct temporal parameters of sensory input. Here we demonstrate that the temporal frequency of a visual stimulus determines the locus of expression and specificity of visual response potentiation. Repetitive high frequency stimulation (HFS, 20 Hz), but not low frequency stimulation (LFS, 2 Hz), suppresses the activity of fast-spiking interneurons, and primes ongoing gamma oscillatory rhythms for visually-evoked phase reset. Accordingly, visual stimulation subsequent to HFS induces a non-stimulus specific response potentiation that is expressed in all cortical layers. In contrast, LFS induces a stimulus specific response potentiation that is specifically expressed in layer 4. This generalized response potentiation induced by HFS is coincident with an improved performance in a visual detection task that generalizes to novel visual stimuli.

Key Words:
visual cortex, oscillations, plasticity

Introduction

Specific frequencies of synaptic stimulation engage enduring changes in synaptic strength that are a primary mechanism for information storage in neural circuits. A wealth of data from brain slices demonstrates that high frequency stimulation induces long-term potentiation (LTP) of excitatory synapses, while low frequency stimulation induces synaptic long-term depression (LTD, Feldman et al., 1999; Huerta and Lisman, 1996; Kirkwood and Bear, 1994; Larson et al., 1986). Tetanic stimulation *in vivo* in animal models reveals a similar dependence of synaptic plasticity on stimulation temporal frequency, with synaptic depression and potentiation induced by low and high frequency stimulation respectively (Cooke and Bear, 2010; Nabavi et al., 2014; Whitlock et al., 2006). Indeed, high frequency tetanic visual stimulation consisting of a 9 Hz full-field flash increases visually evoked responses in humans (McNair et al., 2006) and rats (Clapp et al., 2006). Experiments designed to explore sensory stimulation with temporal frequencies associated with LTP induction, demonstrate that tetanic stimulation induces enhances response amplitude, discrimination and perception in visual, auditory and somatosensory systems (Beste et al., 2011; Brickwedde et al., 2020; Pegado et al., 2016;

Sanders et al., 2018). Potentiation induced by non-invasive sensory stimulation requires NMDA receptors for the expression of sensory changes indicating an LTP like mechanism (Clapp et al., 2006; Dinse et al., 2003).

Interestingly, repetitive low frequency visual stimulation (LFS) also leads to long-lasting changes in visual responses that emerge slowly and require NMDA receptor activation (Cooke et al., 2015). LFS induces robust changes in the output of primary visual cortex (V1) in response to subsequent presentations of the familiar visual stimulus, including a potentiation of layer 4 visual responses, and an increase in the oscillatory power of multiple frequency bands, and requires sleep for expression (Aton et al., 2014; Frenkel et al., 2006; Gavornik and Bear, 2014; Kissinger et al., 2020). This response potentiation occludes subsequent LTP induced by HFS stimulation of thalamus (Cooke and Bear, 2014), and is highly selective for the characteristics of the familiar visual stimulus (Andermann et al., 2010; Aton et al., 2014; Frenkel et al., 2006). Indeed, repetitive low frequency stimulation induces a constellation of changes in rodent primary visual cortex including an increase in the firing rate of regular-spiking (RS) neurons throughout V1, and an increase in the strength of orientation tuning of RS neurons tuned to the familiar stimulus (Cooke and Bear, 2010; Frenkel et al., 2006; Kaplan et al., 2016). The selectivity of visual response potentiation suggests that it is expressed early in the visual pathway (Cooke et al., 2015; Poggio et al., 1992; Zaehle et al., 2007).

In the visual cortex, the power of multiple oscillatory bands increases in layer 4 in response to a familiar low temporal frequency stimulus, leading to the intriguing suggestion that visual stimulus familiarity is encoded by changes in oscillatory power. In concert, the phase of cortical oscillations also regulates the magnitude and perception of incoming visual stimuli (Kim et al., 2007; Kissinger et al., 2018). Indeed, the frequency of incoming auditory and somatosensory stimulation can entrain cortical oscillations and impact perception of subsequent stimuli (Brickwedde et al., 2020; ten Oever et al., 2017). Attention and motivation also increase the power of cortical high frequency oscillations and impact the encoding of short-term memory (Jutras et al., 2009; Montgomery and Buzsáki, 2007) and working memory tasks (Lisman, 2010). Thus, the expression of sensory-evoked synaptic plasticity depends on the time-locked sensory response as well as the magnitude and phase of ongoing cortical oscillations (Brickwedde et al., 2019; Howe et al., 2017; Park et al., 2016).

The selectivity of visual response potentiation following LFS in rodents is modulated by the output of fast spiking interneurons (FS INs) expressing the Ca^{2+} binding protein parvalbumin. Suppression of parvalbumin-expressing interneuron output via optogenetic silencing or the NMDAR antagonist ketamine decreases the selectivity of visual response potentiation (Kaplan et al., 2016). Interestingly, genetic deletion of the immediate early gene neuronal pentraxin 2 (NPTX2; aka NARP) which is highly enriched at excitatory synapses onto parvalbumin-positive interneurons, inhibits the induction of visual response potentiation by a single bout of LFS (Chang et al., 2010; Gu et al., 2013; O'Brien et al., 1999; Xu et al., 2003). However, robust visual response potentiation is induced in $NPTX2^{-/-}$ mice in response to high temporal frequency visual stimulation (HFS, 20 Hz; Gu et al., 2013). This suggests that HFS may over-ride constraints on visual response potentiation imposed by FS IN output.

Here we assess the impact of the temporal frequency of repetitive visual stimulation on long-lasting changes in visual response properties. We find that a single bout of LFS is sufficient to induce an increase in the magnitude of visual responses that is restricted to layer 4 and the experienced visual stimulus. In contrast a single bout of HFS potentiates visual responses throughout V1 in response to familiar and novel stimuli. HFS induces a long-lasting suppression of the output of FS INs and sensitizes cortical gamma oscillations to phase reset by all subsequent visual stimuli. This general enhancement of visual response strength following HFS is paralleled by an increase in performance in a visual detection task.

Methods

Animals. Experiments utilized equal numbers of adult (postnatal day 60-90) male and female C57BL/6J mice (Jackson Lab, Bar Harbor, ME). Subjects were housed on a 12:12 hour dark:light cycle with food and water *ad libitum*, and experiments were initiated ~6 hours into the light phase. All procedures conformed to the guidelines of the University of Maryland Institutional Animal Care and Use Committee. Sample sizes were determined by power analysis of previous studies quantifying the effect of visual experience on visual response amplitudes.

Electrophysiology. House-made 1.2 mm length 16-channel shank electrodes were implanted into binocular V1 (from Bregma: posterior, 2.8 mm; lateral, 3.0 mm; ventral, 1.2 mm) of adult mice, anesthetized with 2.5% isoflurane in 100% O_2, as described (Bridi et al., 2018; Murase et al., 2017). Mice received a single dose of carprofen (5 mg/kg, SQ) for post-surgical analgesia after the return of the righting reflex. One week after surgery and one day before electrophysiological recordings, mice were habituated for 45 minutes to head restraint. Broadband electrophysiological data was collected from awake head-fixed mice, using RZ5 bioamp processor and RA16PA preamp (Tucker Davis Technologies, TDT) and multiunit waveforms sorted into single units using an automatic Bayesian clustering algorithm in OpenSorter (TDT) as described (Murase et al., 2017). Single units (SUs) were processed in MATLAB and classified as regular spiking (RS, presumptive excitatory neurons) or fast spiking (FS IN, presumptive inhibitory neurons) based on waveform slope 0.5 msec after the trough, time between trough and peak, and the ratio of trough to peak height (Niell and Stryker, 2008). VEPs and SUs were assigned to cortical layer based on LFP waveform shape, and current source density calculated with single site spacing from the laminar array (Guo et al., 2017; Mitzdorf, 1985).

Visual Stimulation. Visual stimuli were presented using MATLAB (Mathworks) with Psychtoolbox extensions (Brainard, 1997; Pelli, 1997). Prior to visual stimulation each day mice passively viewed a grey 26 cd/m^2 screen for 200 seconds (spontaneous). Visually evoked responses were recorded in response to 200 x 1s trials of 0.05 cycles per degrees, 100% contrast, square-wave gratings reversing at either 2 Hz (LFS) or 20 Hz (HFS) at various orientations. VEPs and SUs were recorded 24 hours after initial visual stimulation with HFS or LFS, in response to only LFS (200 x 1s trials of 0.05 cycles per degrees, 100% contrast, square-wave gratings reversing at 2 Hz).

Data Analysis. Spike rates of sorted SUs were calculated as the average firing rate during each 1 second epoch (200 trials). Peristimulus-time histograms (PSTH) were calculated for each SU using 5ms bins and smoothed with a gaussian kernel (Kissinger et al., 2018). To examine changes in oscillatory power by frequency, PSTHs were z-scored, and filtered from 1 to 100Hz using a sliding frequency window via a bandpass elliptic filter with a span of 3Hz in MATLAB. The analytic signal of band-passed PSTHs was calculated using a Hilbert transform, and the absolute value was used to calculate power within each frequency band.

Visually evoked potentials (VEPs) were calculated as the trough to peak amplitude of the average of 1 second LFP epochs during visual stimulation in MATLAB, as described (Murase et al., 2017). To examine changes in oscillatory power by frequency and the reliability of incoming visual stimulation to reset the phase of ongoing oscillations (Inter-Trial Phase Consistency, ITPC, a time locked measure of oscillatory phase), spontaneous and evoked LFPs were z-scored then convolved with complex Morlet wavelets from 1 to 100Hz using a 3Hz window (Fiebelkorn et al., 2018). The wavelet cycle width varied with filtered frequency (1-10Hz = 2 cycles, 11-14Hz=3 cycles, 15-20Hz=4 cycles, 21-100Hz=5 cycles). The absolute value of the complex vector was used to calculate oscillatory power. Power was averaged between trials for each subject, and activity is reported as percent change in power relative to spontaneous activity recorded on the first day prior to experimental manipulation (experimental – baseline / baseline x 100). Averaged percent change in evoked power was calculated during the 100-200 ms post stimulus onset, binned oscillatory activity was averaged from this window. Oscillatory bins were defined as: delta 1-4Hz, theta 4-8Hz, alpha 8-13Hz, beta 13-30Hz, and gamma 30-100Hz. The second half of the complex vector was normalized, averaged and the absolute value was used to calculate ITPC. ITPC was binned by oscillatory frequency. Utilizing the calculated oscillatory phase of the LFP, the phase of each frequency for each single unit was calculated then averaged as Spike-Phase Consistency.

Behavior. Psychophysical measurements of spatial acuity were assessed by performance in a 2 alternative forced choice visual detection task. Task training and testing utilized a Bussey-Saksida Touch Screen Chamber (Lafayette Instruments; Horner et al., 2013), with custom plexiglass inserts. An opaque insert divided the LCD touch screen in two vertical halves, for simultaneous display of the correct and incorrect visual stimuli. A transparent insert, parallel to and 6cm from the touch screen, with 2 5x7 cm swing-through doors, defined the choice point for the calculation of visual stimulus spatial frequency (Fig 7A). Naïve adult mice were trained to associate a high contrast (100%), low spatial frequency (0.05 cycles/degree), 45° sinusoidal grating (positive stimulus) with positive reinforcement (strawberry milk and tone, 3kHz, 0.5s) and a grey image of equal luminance (32 cd/m2; negative stimulus) with negative reinforcement (tone, 400 Hz, 2s). Subjects were food deprived for 20 hours a day, with 4 hours of *ad libitum* food access at the end of each training session. A training session consisted of 30 trials, or 45 minutes. To begin a trial, the subject nose poked in the illuminated liquid reward tray at the rear of the chamber, to trigger the presentation of positive and negative visual stimuli.

Contact with the touch screen turned the visual stimulus off. Choosing the positive stimulus resulted in a liquid reward, choosing the negative stimulus resulted in a 2 second tone followed by a 30 second timeout period. Trials were separated by a 10 second intertrial interval, followed by illumination of the liquid reward tray to signal the beginning of a new trial. Criterion was defined as 25/30 correct trials within 45 minutes -83% correct). After reaching criterion, acuity testing was initiated. In acuity testing, the positive stimulus was rotated to a novel orientation (45°+15°), following successful completion (≥ 60%) of a block of 10 trials, the spatial frequency was increased incrementally (0.05 cpd steps). The highest spatial frequency with performance of ≥ 70% correct choices is defined as the subject's visual spatial acuity. Following assessment of initial acuity subjects were randomly divided into 2 groups, half viewed 200 seconds of LFS, while the other half viewed 200 seconds of HFS, at a novel orientation, and returned to their home cage. 24 hours after visual stimulation, acuity was tested at a familiar stimulus orientation (used for LFS or HFS) and at a novel orientation, with test order randomized. Subjects were then returned to food and water *ad libitum* for 2 weeks in the mouse colony. The full sequence was repeated, with novel stimulus orientations, such that individuals that previously received LFS received HFS, and vice versa. There was no difference in initial acuity between the two testing periods (first, 0.33 ± 0.03 cpd; second, 0.29 ± 0.02 cpd, Student's t-test, $p = 0.30$) and groups were combined in the final analysis.

Statistics. Statistical analysis was completed using JASP (JASP Stats). Repeated measures ANOVA (RANOVA) was used to compare LFP data arising from 3 time points within the same subject, including VEP, oscillatory power and ITPC, followed by a Bonferroni *post-hoc* when appropriate. We did not assume that signal from the same electrode was the same single unit over multiple days, therefore, unpaired Student's t-test was used to compare 2 groups and a one-way ANOVA was employed to compare 3 groups, followed by a Tukey *post-hoc* when appropriate. A multivariate ANOVA (MANOVA) with a Bonferroni *post-hoc,* when appropriate, was used to compare oscillatory data consisting 2 time points with multiple frequency bands .To compare the change in oscillatory power within subjects we employed a one-sided Student's t-test with a Bonferroni correction for multiple comparisons. In text, n is reported as the total number of subjects, followed by the total number of recorded single units. Exact p values are reported in the text, except when $p < 0.001$.

Results

Visual stimulus frequency controls plasticity of visual responses

To examine the impact of the temporal frequency of repetitive visual stimulation on the plasticity of visual responses, we examined the magnitude of visually-evoked potentials (VEPs) throughout the depth of the primary visual cortex (V1). Head-fixed awake mice viewed 200 x 1s trials of square-wave gratings (0.05 cycles per degrees, 100% contrast, 60° orientation) delivered at low frequency (2 Hz) or high frequency (20 Hz, Fig. 1). Long lasting visual response potentiation was induced by both protocols, and the location and generalization of visual response potentiation was determined by the visual stimulus temporal frequency. 24 hours after a single bout of low frequency stimulation (LFS), the amplitude of the layer 4 VEP was significantly increased in response to familiar (60°), but not novel (150°) visual stimulus orientations, mimicking the

specificity of stimulus selective response potentiation induced by LFS over multiple days (Frenkel et al., 2006; n = 16, RANOVA$_{(df, 2, 15)}$, Bonferroni *post-hoc*, F = 9.13, p < 0.001; initial v. familiar: p = 0.023, Fig. 1B).

In contrast, 24 hours after a single bout of high frequency stimulation (HFS), the amplitude of VEPs throughout all layers of V1 were significantly increased in response to the familiar (60°) and novel (150°) visual stimulus orientations (n=11, RANOVA $_{(df, 2, 10)}$, Bonferroni *post-hoc*, layer 2/3: F = 5.25, p = 0.015, initial v. familiar p = 0.023, initial v novel p = 0.032; layer 4: F = 7.31, p = 0.004, initial v. familiar p = 0.038, initial v. novel: p = 0.005; layer 5/6: F = 11.41, p < 0.001, initial v. familiar: p = 0.005, initial v. novel: p = 0.022, Fig. 1D). A similar potentiation of VEP amplitudes that generalized to novel stimuli was induced if HFS stimulation preceded or followed the visual stimulation used to assess baseline VEP amplitudes (Between subjects RANOVA $_{(df 1,12)}$ layer 2/3: F = 0.001, p = 0.97, layer 4: F = 0.010, p = 0.92, layer 5: F = 0.00003, p = 0.995, data not shown). HFS also increased VEP amplitudes evoked by visual stimuli of novel spatial frequencies (Fig. S1). Thus, LFS induces a localized and stimulus-specific response potentiation and HFS induces a global and generalized response potentiation.

Visual stimulus frequency acutely modulates oscillation power, phase, and LFP-Spike coupling in V1

VEP amplitudes reflect the interaction between stimulus-evoked neuronal responses and ongoing fluctuations in the cortical local field potential (LFP; Sauseng et al., 2007; Xing et al., 2012). Changes in VEP amplitude could therefore reflect changes in the power or phase of LFP oscillations. To ask how the power of LFP oscillations were impacted during LFS and HFS, we normalized the absolute value of the complex Morlet wavelet convolved LFP during visual stimulation to pre-stimulation spontaneous activity (equal luminant grey screen; 26 cd/m^2). During LFS, low frequency (alpha and beta bands) LFP oscillatory power was significantly increased in all cortical layers (n = 16, one-sided t-test. Layer 2/3: α: t = 4.44, p < 0.001, β: t = 4,39, p < 0.001. Layer 4: α: t = 2.37, p = 0.015, β: t = 2.31, p = 0.024. Layer 5: α: t = 4.07, p < 0.001, β: t = 2.27, p = 0.019, Fig. 2A). Similarly, during HFS, low frequency (delta, alpha and beta bands) power was significantly increased in all layers (n=11, one-sided t-test, layer 2/3; δ: t = 2.42, p = 0.019, α: t = 3.21, p = 0.005, beta, t = 3.57, p = 0.003; layer 4; δ: t = 2.11, p = 0.031, α: t = 2.94, p = 0.008, β: t = 2.82, p = 0.009; layer 5; δ: t = 2.31, p = 0.023, α: t = 1.93, p = 0.042, β: t = 1.92, p = 0.043; Fig. 2C).

To ask how the temporal frequency of visual stimulation impacted the phase of ongoing LFP oscillations, we convolved the LFP signal with a complex Morlet wavelet and calculated the angle of the resultant complex output. Inter-trial phase consistency (ITPC), which ranges from 0 (if phase was random, and not reset by incoming visual input) and 1 (if phase was reset similarly in all trials), was calculated from the time-locked phase and compared to the ITCP during pre-stimulation spontaneous activity. LFS and HFS had differential effects on phase reset of ongoing LFP oscillations. LFS increased phase reset in low frequencies (delta, theta, alpha, and beta) in all cortical layers and increased gamma phase reset in layer 2/3 (n = 16 subjects, Layer 2/3: MANOVA $_{(df, 1, 5)}$ F = 15.94, p < 0.001, δ: F = 36.41, p < 0.001, θ: F = 75.21, p < 0.001, α: F = 88.20, p < 0.001, β: F = 42.22, p < 0.001, γ: F = 4.277, p = 0.047. Layer 4: MANOVA $_{(df, 1, 5)}$ F = 15.98, p < 0.001, δ: F =

45.01, $p < 0.001$, θ: $F = 56.15$, $p < 0.001$, α: $F = 65.05$, $p < 0.001$, β: $F = 39.86$, $p < 0.001$. Layer 5/6: MANOVA $_{(df, 1, 5)}$ $F = 11.10$, $p < 0.001$, δ: $F = 20.59$, $p < 0.001$, θ: $F = 51.07$, $p < 0.001$, α: $F = 46.05$, $p < 0.001$, β: $F = 35.09$, $p < 0.001$). In contrast, HFS significantly increased phase reset of intermediate frequencies (alpha and beta) in all cortical layers, and increased gamma reset in layers 2/3 and 4. Interestingly, HFS decreased delta reset in all cortical layers, with no changes observed in theta power (n = 11 subjects, Layer 2/3: MANOVA $_{(df, 1, 5)}$ $F = 10.46$, $p < 0.001$, δ: $F = 7.76$, $p = 0.011$, α: $F = 16.68$, $p < 0.001$, β: $F = 43.33$, $p < 0.001$, γ: $F = 10.63$, $p = 0.004$. Layer 4: MANOVA $_{(df, 1, 5)}$ $F = 11.26$, $p < 0.001$, δ: $F = 10.09$, $p = 0.005$, α: $F = 28.28$, $p < 0.001$, β: $F = 48.15$, $p < 0.001$, γ: $F = 5.60$, $p = 0.028$. Layer 5/6: MANOVA $_{(df, 1, 5)}$ $F = 6.46$, $p = 0.002$, δ: $F = 5.84$, $p = 0.025$, α: $F = 24.25$, $p < 0.001$, β: $F = 34.24$, $p < 0.001$).

The output of fast spiking cortical interneurons (FS INs) expressing parvalbumin play a fundamental role in the control of sensory evoked LFP amplitudes by influencing the strength of gamma and generation of theta oscillations (Cardin et al., 2009; Sohal et al., 2009; Stark et al., 2013). To quantify the pattern and strength of individual FS IN output during LFS and HFS we calculated the oscillatory power of the post-stimulus time histogram from simultaneously acquired single unit activity. Oscillatory power during visual stimulation was normalized to pre-stimulation spontaneous activity. LFS increased the power of theta (4 - 8 Hz) as well as mid-frequency oscillations (7 - 30 Hz, n = 16 subjects, 23 units. One-sided t-test, θ: $t = 2.22$, $p = 0.016$, α: $t = 2.04$, $p = 0.024$, β: $t = 1.84$, $p = 0.036$). HFS increased the power of alpha and beta frequencies (13 - 30 Hz, n = 11 subjects, 19 units. One-sided t-test, α: $t = 1.81$, $p = 0.039$, β: $t = 2.41$, $p = 0.011$. Fig. 3B&F) demonstrating entrainment of FS IN output to the visual stimulus temporal frequency. To quantify the coherence of FS IN activity with on-going LFP oscillations, we utilized the time-locked LFP phase to examine the consistency of FS IN spiking within each oscillatory frequency during LFS and HFS. LFS significantly increased FS IN firing phase consistency with delta in all cortical layers and theta in layers 2/3 and 4 (Student's t-test, n = 16 subjects, 22 units, layer 2/3: δ: $t = 3.63$, $p < 0.001$, θ: $t = 3.66$, $p < 0.001$, layer 4: δ: $t = 8.10$, $p < 0.001$, θ: $t = 3.87$, $p < 0.001$ layer 5: δ: $t = 2.02$, $p = 0.025$, Fig. 3D). No significant differences in FS IN firing phase consistency were observed during HFS (Fig. 3H).

Changes in oscillatory power do not predict visual response potentiation

Changes in mid frequency LFP oscillations observed in layer 4 have been proposed to encode visual stimulus familiarity (Kissinger et al., 2018). To ask if the familiarity of the visual stimulus used for LFS and HFS are reflected in LFP oscillations, we examined the response to the familiar (60° orientation) and novel (150° orientation) visual stimuli 24 hours after the initial visual stimulation. We utilized the absolute value of the Morlet wavelet convolved LFP in the time window of maximal visually evoked activity (100-200 ms after stimulus reversal). 24 hours after LFS, the familiar visual stimulus induced a significant increase in beta power (13 – 30 Hz) in layers 4 and 5/6 (n = 16, RANOVA $_{(df, 2, 15)}$, Bonferroni *post hoc*. Layer 4: $F = 6.51$, $p = 0.004$, initial v. familiar, $p = 0.004$. Layer 5/6: $F = 3.92$, $p = 0.031$, initial v. familiar: $p = 0.027$). In contrast, 24 hours after HFS, both the familiar and novel stimuli triggered a significant decrease in theta power in all cortical layers (n = 11, RANOVA $_{(df, 2, 10)}$ with Bonferroni *post-hoc*. Layer 2/3: $F = 8.633$, $p = 0.002$; initial v. familiar, p =

0.015, initial v. novel, p=0.003. Layer 4: F = 8.47, p = 0.002; initial v. familiar, p = 0.016, initial v. novel, p = 0.003. Layer 5/6: F = 7.936, p = 0.003, initial v. familiar, p=0.018; initial v. novel, p = 0.004, Fig. 4D). Additionally, HFS induced a significant decrease in delta power in layers 4 and 5/6 in response to the familiar and novel stimuli (n = 11, RANOVA $_{(df, 2, 10)}$ with Bonferroni *post-hoc*. Layer 4: F= 10.24, p < 0.001; initial v familiar, p = 0.031, initial v. novel, p < 0.001. Layer 5/6: F = 7.681, p = 0.003, initial v familiar, p = 0.04, initial v novel, p = 0.003, Fig 4D). Interestingly, the decreases in delta and theta power 24 hours after HFS are also observed in spontaneous activity prior to stimulation with familiar or novel visual stimuli, reflecting the long-term consequence of previous repetitive visual stimulation (Fig. S2E).

Visually-evoked reset of ongoing gamma oscillations predicts visual response potentiation

The phase of on-going LFP oscillations, and their reset in response to visual stimulation, can modify the amplitude of visually-evoked responses (Kim et al., 2007; Kissinger et al., 2018). To ask if visual response potentiation is coincident with visually-induced phase reset of the LFP we calculated the average ITPC during maximum visually-evoked activity (100-200 ms after stimulus onset). 24 hours after LFS, the familiar stimulus induced a significant increase in beta and gamma ITPC that was restricted to layer 4 (n = 16 subjects. RANOVA $_{(df, 2, 15)}$, Bonferroni *post-hoc*, β: F = 5.20, p = 0.011; initial v. familiar: p = 0.045, γ: F = 8.82, p < 0.001; initial v. familiar: p = 0.005, Fig 5B). In contrast, 24 hours after HFS, both familiar and novel visual stimuli induced a significant increase in gamma ITPC in all cortical layers (n = 11 subjects. RANOVA $_{(df, 2, 10)}$, Bonferroni *post-hoc*, layer 2/3: F = 19.42, p < 0.001; initial v. familiar: p = 0.001; initial v. novel: p = 0.003. Layer 4: F = 13.04, p < 0.001; initial v. familiar: p = 0.010; initial v. novel: p = 0.006. Layer 5: F = 5.29, p = 0.025; initial v. familiar: p = 0.022; initial v. novel: p = 0.021, Fig 5D). Thus, the expression of increased gamma ITCP mirrored the locus and specificity of VEP potentiation in response to LFS and HFS.

To ask how changes in FS IN activity reflect response potentiation, we examined the spike rate and oscillatory power of FS INs to the familiar (60° orientation) and novel (150° orientation) visual stimuli 24 hours after LFS or HFS. HFS induced a significant suppression of FS IN firing rates and significantly decreased the power of FS output at frequencies above theta (7 - 100Hz, n=11 subjects, 19 (initial), 20 (familiar), 20 (novel) units. One-way ANOVA $_{(df, 2, 57)}$, Tukey *post-hoc*, F = 4.50, p = 0.015; initial v. familiar: p = 0.022; initial v. novel: p = 0.046. Fig. 6E). Sustained suppression of FS IN firing rates and oscillatory power 24 hours after HFS was also observed in spontaneous activity prior to probe with familiar and novel stimuli (Fig. S2F). There were no significant changes in FS IN firing rate or power following LFS (n = 11 subjects, 19 (initial), 20 (familiar), 20 (novel) units. One-way ANOVA$_{(df, 2, 56)}$, Bonferroni *post-hoc*, α: F = 6.862, p = 0.002, initial v. familiar, p = 0.004, initial v. novel, p = 0.011, β: F = 8.898, p < 0.001, initial v. familiar, p = 0.003, initial v. novel, p = 0.001, γ: F = 5.998, p = 0.004, initial v. familiar, p = 0.009, initial v. novel, p = 0.015; Fig 6F).

We calculated spike-phase consistency between each FS IN and the LFP of each cortical layer to ask how FS IN firing is related to the phase of on-going LFP oscillatory activity. 24 hours after LFS there was no significant change in FS IN spike-LFP-phase consistency in any cortical layer in response to novel or familiar visual

stimuli (n = 16 subjects, 22 (initial), 23 (familiar), 20 (novel) units; Fig 6C & D). In contrast, 24 hours after HFS, presentation of familiar and the novel visual stimuli induced a significant increase in FS IN spike-LFP phase coupling with gamma oscillations across all cortical layers (n = 11 subjects, 19 (initial), 20 (familiar), 20 (novel) units. One-way ANOVA$_{(df, 2, 56)}$, Bonferroni *post-hoc*. Layer 2/3: F = 6.795, p = 0.002, initial v. familiar p = 0.009, initial v. novel p = 0.005. Layer 4: F = 5.655, p = 0.033, initial v. familiar p = 0.008, initial v. novel p = 0.005. Layer 5: F = 6.072, p = 0.004, initial v. familiar p = 0.026, initial v. novel p = 0.006; Fig 6H). Thus, HFS induced a decrease in FS IN firing rates, and an increase in FS IN phase coupling with gamma.

HFS enhances visual acuity

HFS induced an increase in VEP magnitudes and ITPC in response to visual stimuli with novel orientations and spatial frequencies, suggesting a general enhancement of visual function that may be reflected in visual acuity. To test this prediction, we examined the impact of LFS and HFS on spatial acuity assessed by performance in a 2 alternative forced-choice spatial frequency detection task. Naïve mice (n = 12) were trained to associate a liquid reward with a simple visual stimulus (high contrast (100%), low spatial frequency (0.05 cpd, 45° sinusoidal grating). Subjects performed 30 trials per day, requiring 12.3 ± 1.05 days to reach criterion of 25/30 correct trials (83%; Fig 7B). To assess spatial acuity, the positive stimulus was rotated to a novel orientation (45°±15°), and subjects completed blocks of 10 trials with spatial frequencies from 0.05 cpd to 0.7 cpd in increments of 0.05 cpd. Spatial acuity was defined as highest spatial frequency with performance of ≥ 70% correct choices.

Following determination of baseline spatial acuity, subjects passively viewed 200 x 1 second trials of either LFS or HFS at a novel orientation (45° ± 30°). There was no significant difference in baseline spatial acuity between subjects assigned to LFS and HFS groups (average +/- SEM cpd, LFS; 0.33 ± 0.02; HFS 0.30 ± 0.03 cpd, Student's t-test, p = 0.63,Fig. 6C). 24 hours following visual stimulation, visual performance was assessed at the familiar (45° ± 30°) or another novel orientation (45° ± 60°). Following LFS, we observed no change in spatial acuity assessed with the familiar (0.30 ± 0.03 cpd) or novel visual stimulus (0.37 ± 0.03 cpd; n = 12, RANOVA $_{(df, 2, 11)}$, F = 4.02., p = 0.032, initial v familiar p = 0.303, initial v. novel p = 0.303). In contrast, 24 hours after HFS, spatial acuity was significantly enhanced in response to familiar (0.46 ± 0.03 cpd) and novel visual stimulus orientations (0.46 ± 0.03; n = 12, RANOVA $_{(df, 2, 11)}$, Bonferroni *post-hoc*, F = 6.87, p = 0.005; initial v. familiar, p = 0.011; initial v. novel, p = 0.011). Together this demonstrates that HFS induces a sustained, and highly generalizable increase in visual function.

Discussion

The frequency and pattern of synaptic stimulation has long been known to be a decisive parameter in in the induction of long-term changes in synaptic strength, both in brain slices and in response to repetitive sensory or motor stimulation. We show for the first time that temporal frequency of brief visual stimulation determines the location of expression and the specificity of visual response potentiation in mouse V1. HFS suppresses the activity of FS INs, and primes ongoing gamma oscillatory rhythms for visually-evoked phase reset. Accordingly,

visual stimulation subsequent to HFS induces a non-stimulus specific response potentiation that is expressed in all cortical layers. In contrast, LFS induces a stimulus specific response potentiation that is specifically expressed in layer 4. Importantly, relatively brief HFS is sufficient to induce sustained, generalized enhancement of visual responses in mouse V1, and an improved performance in a visual detection task. These results suggest the potential for the use of non-invasive, high-frequency sensory stimulation to broadly improve visual perception.

Robust visual response potentiation was first described in the mouse visual cortex following hundreds of repetitions of LFS over days (Andermann et al., 2010; Aton et al., 2014; Frenkel et al., 2006). This stimulus-selective response potentiation (SSRP) is expressed in layer 4 VEP, and is highly selective for the orientation, contrast and spatial frequency of the visual stimulus used for induction. Indeed, response potentiation is not seen following rotation of the orientation of the visual stimulus by as little as 5 degrees (Cooke and Bear, 2010). We show that a single, shorter duration bout of LFS (1s x 200 presentations) is sufficient to engage response potentiation of layer 4 VEPs, with similar specificity but smaller magnitude than that induced by repetitive LFS over several days (Frenkel et al., 2006). In contrast, HFS-induced response potentiation is expressed as an increase in VEP amplitudes in all layers of V1 and generalizes to novel visual stimuli. HFS decreased spontaneous and visually-evoked activity of FS INs in V1, and primed the visual cortex for gamma phase reset by all subsequent visual stimulation.

It is increasingly appreciated that V1 encodes much more than the statistics of the visual stimulus. For example, V1 can replay complex temporal sequences of visual stimulation (Han et al., 2008; Yao et al., 2007), encode familiarity of individual stimuli and sequences (Frenkel et al., 2006; Gavornik and Bear, 2014) and encode the timing of visually-cued reward (Zold and Hussain Shuler, 2015). Work in animal models and human subjects demonstrate that plasticity of these representations can be modulated by non-visual stimulation and enhanced with visual training or repetitive visual stimulation. Spontaneous and evoked activity in V1 are also modulated by changes in cortical oscillatory rhythms induced by locomotion (Niell and Stryker, 2010), generalized motor movements, behavioral state (Stringer et al., 2019) and input from other sensory systems (Iurilli et al., 2012). Indeed, reward timing is encoded by an increase in the 5 - 10 Hz (theta) frequency power (Zold and Hussain Shuler, 2015). Changes in V1 beta (12 - 30 Hz) and gamma (30 - 100 Hz) power are induced by visual stimulation in awake mice (Niell and Stryker, 2010; Saleem et al., 2017; Veit et al., 2017). Furthermore, an increase in the visually-evoked power of theta (4 - 8 Hz), alpha (8 - 12 Hz) and beta (12 - 30 Hz) oscillations emerges in layer 4 of rodent V1 following repetitive visual stimulation with a familiar stimulus (Kissinger et al., 2018). We observed a similar increase in beta (13 - 30 Hz) oscillatory power following LFS in cortical layers 4 and 5 in response to familiar stimuli, and an increase in alpha (7- 13 Hz) power in layer 4. We did not probe for encoding of the temporal frequency of the initial HFS and LFS. However, HFS induced a decrease in spontaneous low frequency power (1 – 8 Hz) in all cortical layers, that was also observed in response to stimuli with novel and familiar orientation. HFS also decreased the firing rate of FS INs and decreases spontaneous and visually evoked theta power across all cortical layers, consistent with the role of

FS INs in the generation of theta oscillations within the cortex (Stark et al., 2013) and hippocampus (Buzsáki, 2002).

Changes in oscillatory power in the absence of phase synchronization could also be expected to reduce response magnitude by increasing variability, while phase synchronization would increase response magnitude and decrease response variability. Indeed, visually-induced phase reset of gamma oscillations predicts both the location and specificity of visual response potentiation: all visual stimuli subsequent to HFS reset the phase of ongoing gamma oscillations throughout V1 and familiar visual stimuli subsequent to LFS induced gamma phase reset in layer 4. The ability to prime gamma oscillations for visually-evoked phase reset may be due to specifics of generation and modulation. Cortical gamma oscillations are generated by feedforward thalamo-cortical connections (Bastos et al., 2015; van Kerkoerle et al., 2014; Saleem et al., 2017; Spaak et al., 2012), while gamma power and phase synchrony are modulated/ entrained by the output of cortical PV INs (Cardin et al., 2009; Chen et al., 2017; Sohal et al., 2009). The enhanced sensitivity to gamma phase reset by visual stimulation and enhanced generalizability of response potentiation are consistent with a reduced influence of FS IN output on gamma following HFS (Kaplan et al., 2016).

Indeed, the temporal frequency of the initial visual stimulation was reflected in the increase in oscillatory power and phase reset during initial stimulation, as well as in the increase in oscillatory power of FS INs. LFS and HFS will recruit activity in different subsets of neurons in mouse V1, tuned to lower and higher temporal frequencies respectively (Gao et al., 2010). 20 Hz visual stimulation (HFS) is also close to flicker fusion in the murine visual system, and may therefore drive the largest number of neurons to spike at high frequency (Durand et al., 2016; Porciatti et al., 1999; Tanimoto et al., 2015). The HFS induced suppression of FS IN firing rates, and increased FS-gamma oscillation synchrony are not observed during the HFS, suggesting additional processes are necessary for the expression observed at 24 hours. One possibility is that sleep is necessary to consolidate long term changes in cortical activity induced by HFS, as has been shown for stimulus selective response potentiation following LFS (Aton et al., 2014).

The stimulus selective potentiation of layer 4 VEPs induced by days of repetitive low frequency stimulation, and parallel changes in a behavioral response to familiar visual stimuli (vidget) are both inhibited by cortical delivery of NMDAR antagonists and PKM-zeta inhibitor peptide (Cooke et al., 2015). It is not yet known if the generalized visual response potentiation observed in all cortical layers of V1 following HFS is sufficient to drive the increase in spatial acuity demonstrated in visual task performance. Accordingly, we cannot rule out the possibility that the synaptic changes underlying the general increase in spatial acuity following HFS may reflect plasticity in secondary visual areas such as the latero-intermediate area, where neurons are tuned to higher temporal and spatial frequencies than V1 (Marshel et al., 2011).

Our findings provide mechanistic into the cellular and circuit level response of the mouse visual cortex to high (HFS) and low (LFS) frequency repetitive visual stimulation, which may translate to other species including

humans. High frequency (20Hz) flicker of sinusoidal gratings induces a long-lasting improvement in orientation discrimination in human subjects (Beste et al., 2011; Marzoll et al., 2018). Similarly, 20Hz, but not 1 Hz, presentation of an oriented bar improved orientation discrimination (Marzoll et al., 2018). Perceptual improvements via stimulation with a high temporal frequency stimulus are not limited to the visual domains, as 10Hz flickering visual stimulation presented during a word recognition task improved word recall (Williams, 2001; Williams et al., 2006). Trans-cranial brain stimulation techniques including direct current stimulation (tDCS), alternating current stimulation (tACS), and repetitive transcranial magnetic stimulation (rTMS) also alter performance on sensory and memory tasks. Indeed, rTMS stimulation over the visual cortex in cats with a pulse frequency of 1-3 Hz induced transient depression of the amplitude of visual response amplitudes, while a temporal frequency of 10 Hz transiently potentiated visual responses (Aydin-Abidin et al., 2006). The HFS protocol presented here overcomes the transience and stimulus-selectivity of many other stimulation protocols and may be a useful avenue to pursue for rapid, non-invasive vision therapy.

Acknowledgements

This work was supported by the National Institutes of Health grant EY016431 and EY025922 to EMQ.

Figure Legends

Figure 1. LFS and HFS differentially impact the location and generalization of visual response potentiation. A) Experimental timeline: naïve subjects received low frequency visual stimulation (LFS, green: 200 presentations of 0.05 cpd, 100% contrast gratings, 60° orientation, 2 Hz). The initial response is reported as baseline VEP. After 24 hours, VEPs were evoked by familiar and novel visual stimulus orientations presented at 2 Hz. B) Significant increase in VEP amplitude in layer 4 in response to familiar, but not novel, stimulus orientations (RANOVA $_{(df, 2, 15)}$, $F = 9.13$, $p < 0.001$; * = Bonferroni *post hoc* $p < 0.05$; n=16 subjects). C) Timeline, as in A, except that naïve subjects received high frequency visual stimulation (HFS, purple: 200 presentations of 0.05 cycle per degree, 100% contrast grating, 30° orientation, 20 Hz) after initial assessment of baseline VEP. After 24 hours, VEPs were evoked by familiar and novel visual stimulus orientations presented at 2 Hz. D) Significant increase in VEP amplitudes in layers 2/3, 4, and 5/6 in response to familiar and novel stimulus orientations (RANOVA $_{(df, 2, 10)}$, layer 2/3: $F = 5.25$, $p = 0.015$, layer 4: $F = 7.31$, $p = 0.004$; layer 5/6: $F = 11.41$, $p < 0.001$; * = Bonferroni *post hoc* $p<0.05$; n = 11 subjects).

Figure 2. Distinct acute impact of LFS and HFS on oscillatory power and evoked phase reset. Top, green, during LFS: A) Left; average oscillatory power (heat map) from 0-100 Hz (3 Hz bins; y axis) over time (x axis) by cortical layer during LFS. Power was normalized to spontaneous activity in response to 26 cd/m^2 grey screen. Right; significant increase in average α and β power (y axis) across all cortical layers, in δ power in layers 2/3 and 4, and in θ power in layers 2/3 and 5/6 during LFS (one-sided t-test, Grey highlight = $p < 0.05$, n = 16). Power binned by frequency band (δ: 1-4, θ: 4-8, α: 8-13, β: 13-30, γ: 30-100Hz). B) Left; average inter-trial phase consistency during LFS (ITPC; heat map) from 0-100 Hz (in 3 Hz bins; y axis) over time (x axis),

trial averaged. Right; a significant increase in ITPC at all frequencies in layer 2/3 ($MANOVA_{(df, 1, 5)}$, $F = 15.94$, $p < 0.001$), and an increase in all frequencies below gamma in layers 4 ($MANOVA_{(df, 1, 15)}$, $F = 15.98$, $p < 0.001$) and 5/6 ($MANOVA_{(df, 1, 15)}$, $F = 11.10$, $p < 0.001$) during LFS (solid line), relative to spontaneous activity (dashed line). Grey highlight = Bonferroni *post hoc* $p < 0.05$; n = 16 subjects. Bottom, purple, during HFS: C) Left; average oscillatory power (heat map) from 0-100 Hz (3 Hz bins; y axis) over time (x axis) by cortical layer during HFS, normalized as in A. Right; HFS evoked a significant increase in average δ, α and β power in all cortical layers and in θ power in layer 2/3 (one-sided t-test, Grey highlight = $p < 0.05$, n = 11). D) Left; average inter-trial phase consistency during HFS (ITPC; heat map) from 0-100 Hz (in 3 Hz bins; y axis) over time (x axis), trial averaged as in A. Right; HFS (purple line) induced significant changes in ITPC in all cortical layers, including a significant increase in visually driven phase reset in α, and β oscillations (layer 2/3: $MANOVA_{(df, 1, 10)}$, $F = 14.14$, $p < 0.001$, layer 4: $MANOVA_{(df, 1, 10)}$, $F = 12.284$, $p < 0.001$, layer 5: $MANOVA_{(df, 1, 10)}$, $F = 9.95$, $p = 0.0017$), and a significant decrease in the δ oscillation in all layers, relative to spontaneous activity (dashed line). Grey highlight = Bonferroni *post hoc* $p < 0.05$; n = 11 subjects.

Figure 3. Distinct acute impact of LFS and HFS on FS IN oscillatory power and LFP phase synchrony. Top, green, during LFS: A) Heat map depicting PSTH for each FS IN. B) Average change in oscillatory power of FS INs during LFS, binned by frequency band (δ: 1-4, θ: 4-8, α: 8-13, β: 13-30, γ: 30-100Hz, n = 16 subjects). Significant increase in power of θ, α, and β oscillations in FS IN during LFS (one sided t-test with Bonferroni correction, grey highlight = $p<0.05$). C) Heat map of FS IN spike-LFP phase consistency during LFS for each FS IN compared to LFP of each layer. D) Average +/- SEM FS IN spike-LFP phase consistency during LFS (green) compared to spontaneous activity (grey), by frequency. LFS increases FS IN spike-phase consistency with δ oscillations in all cortical layers and with θ in layers 2/3 and 4 (Student's t-test, grey highlight = $p < 0.05$, n = 16 subjects). Bottom, purple, during HSF: E) Heat map depicting PSTH for each FS IN. F) Average change in oscillatory power of FS IN spiking during HFS, power binned by frequency band (δ 1-4, θ: 4-8, α: 8-13, β: 13-30, γ: 30-100Hz, n = 11 subjects). Significant increase in power of α and β oscillations in FS INs during HFS (one sided t-test, grey highlight = $p < 0.05$). G) Heat map of FS IN spike-LFP phase consistency during HFS for each FS IN compared to LFP of each layer. H) Average +/- SEM FS INs spike-LFP phase consistency during HFS (purple) compared to spontaneous (grey) by frequency. HFS does not change FS IN spike-phase consistency in any cortical layer (n = 11 subjects).

Figure 4. LFS and HFS differentially impact oscillatory power during subsequent visual stimulation. Top, green, after LFS: A) Left; average oscillatory power (heat map) from 0 –100 Hz (3 Hz bins; y axis) over time (x axis) across cortical layers during initial visual stimulation, and presentation of familiar and novel visual stimuli 24 hours after LFS. Power is normalized to spontaneous activity during viewing of a 26 cd/m^2 grey screen. Arrowhead indicates stimulus onset, white box indicates time window for assessment of change in oscillatory power (100-200 ms after stimulus onset). B) Average +/- SEM change in oscillatory power, binned by frequency band (δ: 1-4, θ: 4-8, α: 8-13, β: 13-30, γ: 30-100 Hz) during presentation of initial (black), familiar (red), and novel (blue) visual stimuli. In layer 4 and 5/6, a significant increase in average β power in response

to familiar (red) but not novel (blue) visual stimuli relative to initial (black, RANOVA $_{(df, 2, 15)}$, layer 4: F = 6.51, p = 0.004; layer 5/6: F = 3.92, p = 0.031). Grey highlight = Bonferroni *post hoc* p < 0.05; n = 16 subjects. Bottom, purple, after HFS: C) Average oscillatory power (heat map) from 0-100 Hz (3Hz bins; y axis) over time (x axis) across cortical layers during initial visual stimulation, and presentation of familiar and novel visual stimuli 24 hours after HFS. Power normalized as in A. Arrowhead indicates stimulus onset, white box indicates time window for assessment of change in oscillatory power (100-200 ms after stimulus reversal). D) Average +/- SEM change in oscillatory power, binned by frequency band during presentation of initial (black), familiar (red), and novel (blue) visual stimuli. In all layers, a significant decrease in average θ power in response to novel (blue) and familiar (red) visual stimulus, relative to initial (black, RANOVA $_{(df, 2, 10)}$, layer 2/3: F = 8.63, p = 0.002, layer 4: F = 8.47, p = 0.002, layer 5: F = 7.936, p = 0.003). Grey highlight = Bonferroni *post hoc* p < 0.05; n = 11 subjects.

Figure 5. ITPC co-varies with visual response potentiation. Top, green, after LFS: A) Average inter-trial phase consistency 24 hours after LFS in response to initial, familiar and novel visual stimuli (ITPC; heat map) from 0-100 Hz (in 3 Hz bins; y axis) over time (x axis). Trial averaged from complex Morlet wavelet convolution. Arrowhead indicates stimulus onset; white box indicates time window for assessment of change in ITPC (100-200 ms after stimulus onset). B) Average ITPC power binned by frequency band (δ: 1-4, θ: 4-8, α: 8-13, β: 13-30, γ: 30-100Hz) in response to initial (black), familiar (red), and novel (blue) visual stimuli. 24 hours after LFS, the familiar visual stimulus induced a significant increase in layer 4 phase reset of β and γ oscillations relative to initial (black, RANOVA $_{(df, 2, 15)}$, β: F = 5.20, p = 0.011, γ: F = 8.82, p < 0.001). Grey highlight = Bonferroni *post hoc* p < 0.05; n = 16 subjects. Bottom, purple, after HFS: C) Average ITPC 24 hours after HFS in response to initial, familiar and novel visual stimuli (ITPC; heat map) from 0-100 Hz (in 3 Hz bins; y axis) over time (x axis). Trial averaged from complex Morlet wavelet convolution. Arrowhead indicates stimulus onset; white box indicates time window for assessment of change in ITPC (100-200 ms after stimulus reversal). D) Average ITPC power binned by frequency band (δ: 1-4, θ: 4-8, α: 8-13, β: 13-30, γ: 30-100Hz) in response to initial (black), familiar (red), and novel (blue) visual stimuli. 24 hours after HFS, familiar (red) and novel (blue) visual stimuli induced a significant increase in γ oscillatory phase reset in all cortical layers relative to initial (black, RANOVA $_{(df, 2, 10)}$, layer 2/3: F = 19.42, p < 0.001, layer 4: F = 13.04, p < 0.001, layer 5: F = 5.29, p = 0.025). Grey highlight = Bonferroni *post hoc* p < 0.05; n = 11 subjects.

Figure 6. HFS decreases FS IN firing rates and power and increases FS IN spike-and LFP gamma phase consistency. Top, green, after LFS: A) No change in average spike rates of FS IN during presentation of familiar or novel visual stimuli 24 hours after LFS. B) No change in FS IN oscillatory power during presentation of familiar (red, top) or novel (blue, bottom) visual stimuli relative to initial (black). C) Heat map of spike-phase consistency of FS INs in response to initial, familiar and novel visual stimuli by cortical layer from 0 - 100 Hz during the 1000-200 ms following stimulus onset in subjects that received LFS. D) Average FS IN-LFP spike-phase consistency by cortical layer in response to initial (black), familiar (red), and novel (blue) stimuli. No significant difference in spike-phase consistency following LFS. Bottom, purple, after HFS: E) 24 hours after

HFS, both familiar and novel visual stimuli significantly decreased average FS IN spike rate (ANOVA $_{(df, 2, 56)}$, F = 4.50, p = 0.015). * = Tukey *post hoc* p < 0.05; n = 11 subjects. F) Average change in FS IN power by frequency induced by initial (black) and familiar (red) visual stimuli. 24 hours after HFS, familiar and novel stimuli induced a significant decrease in the oscillatory power of FS IN across multiple frequencies (7-100Hz) compared to initial (black; ANOVA$_{(df, 2, 56)}$, α: F = 6.862, p = 0.002, β: F = 8.898, p = 0.0004, γ: F = 5.998, p = 0.004). Grey highlight = Bonferroni *post hoc* p < 0.05, n = 11 subjects. G) Heat map of spike- phase consistency of FS IN during presentation of initial, familiar and novel stimuli by cortical layer from 0-100 Hz during the 100ms following stimulus reversal in subjects that received HFS. H) Average FS IN spike-LFP phase consistency by cortical layer induced by initial (black), familiar (red), and novel (blue) stimuli. 24 hours after HFS, familiar and novel visual stimuli induced a significant increase in FS IN spike-LFP γ phase consistency in all cortical layers (ANOVA$_{(df, 2, 56)}$, Layer 2/3: F = 6.795, p = 0.002, layer 4: F = 5.655, p = 0.006, layer 5: F = 6.072, p = 0.004). Grey highlight = Bonferroni *post hoc* p < 0.05; n = 11 subjects.

Figure 7. HFS enhances visual acuity. A) Left: timeline, subjects were trained in a 2-alternative forced choice visual detection task. Following training, baseline visual acuity was assessed using a novel stimulus orientation and followed by LFS or HFS. Spatial acuity was tested again 24 hour later. Right: cartoon depicting modified Bussey chamber with plexiglass divider introducing a choice point for the assessment of stimulus spatial frequency. B) All subjects reached task criterion of 25/30 correct trials by 18 days of training. C) No significant difference in initial visual acuity prior to the delivery of LFS or HFS (Student's t-test, p = 0.63). D) Average frequency of seeing curves for initial (black), novel (blue) and familiar (red) visual stimulus orientations in subjects that received LFS (green box). E) No significant difference in spatial acuity probed with initial (black, before LFS), novel (blue, after LFS) and familiar (red, after LFS) visual stimulus orientations (n = 12). F) Average frequency of seeing curves for initial (black), novel (blue) and familiar (red) visual stimulus orientations in subjects that received HFS (purple box). G) Spatial acuity probed with novel (blue, after HFS) and familiar (red, after HFS) visual stimulus orientations was significantly increased following HFS (black, before HFS; RANOVA $_{(df, 2, 11)}$, F = 6.817, p = 0.005). * = Bonferroni *post hoc* p < 0.05; n = 12.

Figure S1. HFS enhances VEP amplitudes evoked by novel spatial frequencies. Following HFS, a significant increase in layer 4 VEP amplitudes in response to visual stimuli with a novel orientation, across a range of spatial frequencies (purple) compared to LFS. (Between groups RANOVA$_{(df,6,1)}$, F = 5.88, p = 0.035). * = p < 0.05; n = 9 (HFS), 6 (LFS) subjects.

Figure S2. Distinct sustained effects of LFS and HFS on spontaneous oscillatory power and FS IN spiking. Top, green, after LFS: A) Heat map, average change in spontaneous oscillatory power 24 hours after LFS (% change from pre-stimulation spontaneous activity) from 0-100 Hz (3 Hz bins; y axis) over time (x axis) by cortical layer. B) Average % change in spontaneous oscillatory power 24 hours after LFS, binned by frequency band (δ: 1-4, θ: 4-8, α: 8-13, β: 13-30, γ: 30-100Hz). No change in spontaneous oscillatory power 24 hours after LFS in any cortical layer (n = 16). C) Top, average +/- SEM time-histogram of FS INs, pre (black)

and 24 hours post LFS (green). Middle, average FS IN spike rates pre (black) and 24 hours post LFS (green). Bottom, no change in oscillatory power of FS IN spontaneous activity 24 hours post LFS, binned by frequency band. Significant decrease in θ, β, and γ oscillatory power 24 hours after LFS. Bottom, purple, after HFS: D) Heat map, average change in spontaneous oscillatory power 24 hours after HFS (% change from pre-HFS spontaneous activity) from 0 to 100Hz (3 Hz bins; y axis) over time (x axis) by cortical layer. E) Average % change in spontaneous oscillatory power 24 hours after HFS, binned by frequency band. 24 hours after HFS, δ power is significantly decreased in all layers (one sided t-test, grey highlight = $p < 0.05$; n = 11). F) Top, average +/- SEM time-histogram of FS INs pre LFS (blank) and 24 hours post HFS (purple). Middle, Significant decrease in average FS IN firing rates 24 hours after HFS (unpaired t-test, * = $p < 0.05$; n = 19 (pre), 18 (post) units, 11 subjects). Bottom, average change in spontaneous oscillatory power of FS INs 24 hours post LFS, binned by frequency band. Significant decrease in all frequency bands above δ 24 hours after HFS (One-sided t-test, grey highlight = $p < 0.05$; n = 18 units, 11 subjects).

References

Andermann, M.L., Kerlin, A.M., and Reid, C. (2010). Chronic cellular imaging of mouse visual cortex during operant behavior and passive viewing. Front. Cellullar Neurosci. *4*, 3.

Aton, S.J., Suresh, A., Broussard, C., and Frank, M.G. (2014). Sleep Promotes Cortical Response Potentiation Following Visual Experience. Sleep *37*, 1163–1170.

Aydin-Abidin, S., Moliadze, V., Eysel, U.T., and Funke, K. (2006). Effects of repetitive TMS on visually evoked potentials and EEG in the anaesthetized cat: dependence on stimulus frequency and train duration. J. Physiol. *574*, 443–455.

Bastos, A.M., Vezoli, J., Bosman, C.A., Schoffelen, J.-M., Oostenveld, R., Dowdall, J.R., De Weerd, P., Kennedy, H., and Fries, P. (2015). Visual Areas Exert Feedforward and Feedback Influences through Distinct Frequency Channels. Neuron *85*, 390–401.

Beste, C., Wascher, E., Güntürkün, O., and Dinse, H.R. (2011). Improvement and Impairment of Visually Guided Behavior through LTP- and LTD-like Exposure-Based Visual Learning. Curr. Biol. *21*, 876–882.

Brainard, D.H. (1997). The Psychophysics Toolbox. Spat. Vis. *10*, 433–436.

Brickwedde, M., Krüger, M.C., and Dinse, H.R. (2019). Somatosensory alpha oscillations gate perceptual learning efficiency. Nat. Commun. *10*, 263.

Brickwedde, M., Schmidt, M.D., Krüger, M.C., and Dinse, H.R. (2020). 20 Hz Steady-State Response in Somatosensory Cortex During Induction of Tactile Perceptual Learning Through LTP-Like Sensory Stimulation. Front. Hum. Neurosci. *14*, 257.

Bridi, M.C.D., de Pasquale, R., Lantz, C.L., Gu, Y., Borrell, A., Choi, S.-Y., He, K., Tran, T., Hong, S.Z., Dykman, A., et al. (2018). Two distinct mechanisms for experience-dependent homeostasis. Nat. Neurosci. *21*, 1.

Buzsáki, G. (2002). Theta oscillations in the hippocampus. Neuron *33*, 325–340.

Cardin, J.A., Carlén, M., Meletis, K., Knoblich, U., Zhang, F., Deisseroth, K., Tsai, L.-H., and Moore, C.I. (2009). Driving fast-spiking cells induces gamma rhythm and controls sensory responses. Nature *459*, 663–667.

Chang, M.C., Park, J.M., Pelkey, K.A., Grabenstatter, H.L., Xu, D., Linden, D.J., Sutula, T.P., McBain, C.J., and Worley, P.F. (2010). Narp regulates homeostatic scaling of excitatory synapses on parvalbumin-expressing interneurons. Nat. Neurosci. *13*, 1090–1097.

Chen, G., Zhang, Y., Li, X., Zhao, X., Ye, Q., Lin, Y., Tao, H.W., Rasch, M.J., and Zhang, X. (2017). Distinct Inhibitory Circuits Orchestrate Cortical beta and gamma Band Oscillations. Neuron *96*, 1403-1418.e6.

Clapp, W.C., Eckert, M.J., Teyler, T.J., and Abraham, W.C. (2006). Rapid visual stimulation induces N-methyl-D-aspartate receptor-dependent sensory long-term potentiation in the rat cortex. Neuroreport *17*, 511–515.

Cooke, S.F., and Bear, M.F. (2010). Visual experience induces long-term potentiation in the primary visual cortex. J. Neurosci. *30*, 16304–16313.

Cooke, S.F., and Bear, M.F. (2014). How the mechanisms of long-term synaptic potentiation and depression serve experience-dependent plasticity in primary visual cortex. Philos. Trans. R. Soc. B Biol. Sci. *369*, 20130284.

Cooke, S.F., Komorowski, R.W., Kaplan, E.S., Gavornik, J.P., and Bear, M.F. (2015). Visual recognition memory, manifested as long-term habituation, requires synaptic plasticity in V1. Nat. Neurosci. *18*, 262–271.

Dinse, H.R., Ragert, P., Pleger, B., Schwenkreis, P., and Tegenthoff, M. (2003). Pharmacological modulation of perceptual learning and associated cortical reorganization. Science (80-.). *301*, 91–94.

Durand, S., Iyer, R., Mizuseki, K., De Vries, S., Mihalas, S., and Reid, R.C. (2016). A comparison of visual response properties in the lateral geniculate nucleus and primary visual cortex of awake and anesthetized mice. J. Neurosci. *36*, 12144–12156.

Feldman, D.E., Nicoll, R.A., and Malenka, R.C. (1999). Synaptic plasticity at thalamocortical synapses in developing rat somatosensory cortex: LTP, LTD, and silent synapses. J. Neurobiol. *41*, 92–101.

Fiebelkorn, I.C., Pinsk, M.A., and Kastner, S. (2018). A Dynamic Interplay within the Frontoparietal Network Underlies Rhythmic Spatial Attention. Neuron *99*, 842-853.e8.

Frenkel, M.Y., Sawtell, N.B., Diogo, A.C., Yoon, B., Neve, R.L., and Bear, M.F. (2006). Instructive effect of visual experience in mouse visual cortex. Neuron *51*, 339–349.

Gao, E., DeAngelis, G.C., and Burkhalter, A. (2010). Parallel input channels to mouse primary visual cortex. J. Neurosci. *30*, 5912–5926.

Gavornik, J.P., and Bear, M.F. (2014). Learned spatiotemporal sequence recognition and prediction in primary visual cortex. Nat. Neurosci. *17*, 732–737.

Gu, Y., Huang, S., Chang, M.C., Worley, P., Kirkwood, A., and Quinlan, E.M. (2013). Obligatory role for the immediate early gene NARP in critical period plasticity. Neuron *79*, 335.

Guo, W., Clause, A.R., Barth-Maron, A., and Polley, D.B. (2017). A Corticothalamic Circuit for Dynamic Switching between Feature Detection and Discrimination. Neuron *95*, 180-194.e5.

Han, F., Caporale, N., and Dan, Y. (2008). Reverberation of Recent Visual Experience in Spontaneous Cortical Waves. Neuron *60*, 321–327.

Horner, A.E., Heath, C.J., Hvoslef-Eide, M., Kent, B.A., Kim, C.H., Nilsson, S.R.O., Alsiö, J., Oomen, C.A., Holmes, A., Saksida, L.M., et al. (2013). The touchscreen operant platform for testing learning and memory in rats and mice. Nat. Protoc. *8*, 1961–1984.

Howe, W.M., Gritton, H.J., Lusk, N.A., Roberts, E.A., Hetrick, V.L., Berke, J.D., and Sarter, M. (2017). Acetylcholine Release in Prefrontal Cortex Promotes Gamma Oscillations and Theta-Gamma Coupling during Cue Detection. J. Neurosci. *37*, 3215–3230.

Huerta, P.T., and Lisman, J.E. (1996). Low-frequency stimulation at the troughs of θ-oscillation induces long-term depression of previously potentiated CA1 synapses. J. Neurophysiol. *75*, 877–884.

Iurilli, G., Ghezzi, D., Olcese, U., Lassi, G., Nazzaro, C., Tonini, R., Tucci, V., Benfenati, F., and Medini, P. (2012). Sound-Driven Synaptic Inhibition in Primary Visual Cortex. Neuron *73*, 814–828.

Jutras, M.J., Fries, P., and Buffalo, E.A. (2009). Gamma-band synchronization in the macaque hippocampus

and memory formation. J. Neurosci. *29*, 12521–12531.

Kaplan, E.S., Cooke, S.F., Komorowski, R.W., Chubykin, A.A., Thomazeau, A., Khibnik, L.A., Gavornik, J.P., and Bear, M.F. (2016). Contrasting roles for parvalbumin-expressing inhibitory neurons in two forms of adult visual cortical plasticity. Elife *5*.

van Kerkoerle, T., Self, M.W., Dagnino, B., Gariel-Mathis, M.-A., Poort, J., van der Togt, C., and Roelfsema, P.R. (2014). Alpha and gamma oscillations characterize feedback and feedforward processing in monkey visual cortex. Proc. Natl. Acad. Sci. U. S. A. *111*, 14332–14341.

Kim, Y.J., Grabowecky, M., Paller, K.A., Muthu, K., and Suzuki, S. (2007). Attention induces synchronization-based response gain in steady-state visual evoked potentials. Nat. Neurosci. *10*, 117–125.

Kirkwood, A., and Bear, M.F. (1994). Homosynaptic long-term depression in the visual cortex. J. Neurosci. *14*, 3404–3412.

Kissinger, S.T., Pak, A., Tang, Y., Masmanidis, S.C., and Chubykin, A.A. (2018). Oscillatory Encoding of Visual Stimulus Familiarity. J. Neurosci. *38*, 6223–6240.

Kissinger, S.T., Wu, Q., Quinn, C.J., Anderson, A.K., Pak, A., and Chubykin, A.A. (2020). Visual Experience-Dependent Oscillations and Underlying Circuit Connectivity Changes Are Impaired in Fmr1 KO Mice. Cell Rep. *31*, 107486.

Larson, J., Wong, D., and Lynch, G. (1986). Patterned stimulation at the theta frequency is optimal for the induction of hippocampal long-term potentiation. Brain Res. *368*, 347–350.

Lisman, J. (2010). Working Memory: The Importance of Theta and Gamma Oscillations. Curr. Biol. *20*, R490–R492.

Marshel, J.H., Garrett, M.E., Nauhaus, I., and Callaway, E.M. (2011). Functional specialization of seven mouse visual cortical areas. Neuron *72*, 1040–1054.

Marzoll, A., Saygi, T., and Dinse, H.R. (2018). The effect of LTP- and LTD-like visual stimulation on modulation of human orientation discrimination. Sci. Rep. *8*, 16156.

McNair, N.A., Clapp, W.C., Hamm, J.P., Teyler, T.J., Corballis, M.C., and Kirk, I.J. (2006). Spatial frequency-specific potentiation of human visual-evoked potentials. Neuroreport *17*, 739–741.

Mitzdorf, U. (1985). Current source-density method and application in cat cerebral cortex: investigation of evoked potentials and EEG phenomena. Physiol. Rev. *65*, 37–100.

Montgomery, S.M., and Buzsáki, G. (2007). Gamma oscillations dynamically couple hippocampal CA3 and CA1 regions during memory task performance. Proc. Natl. Acad. Sci. U. S. A. *104*, 14495–14500.

Murase, S., Lantz, C.L., and Quinlan, E.M. (2017). Light reintroduction after dark exposure reactivates plasticity in adults via perisynaptic activation of MMP-9. Elife *6*.

Nabavi, S., Fox, R., Proulx, C.D., Lin, J.Y., Tsien, R.Y., and Malinow, R. (2014). Engineering a memory with LTD and LTP. Nature *511*, 348–352.

Niell, C.M., and Stryker, M.P. (2008). Highly selective receptive fields in mouse visual cortex. J. Neurosci. *28*, 7520–7536.

Niell, C.M., and Stryker, M.P. (2010). Modulation of visual responses by behavioral state in mouse visual cortex. Neuron *65*, 472–479.

O'Brien, R.J., Xu, D., Petralia, R.S., Steward, O., Huganir, R.L., and Worley, P. (1999). Synaptic clustering of AMPA receptors by the extracellular immediate-early gene product Narp. Neuron *23*, 309–323.

ten Oever, S., Schroeder, C.E., Poeppel, D., Van Atteveldt, N., Mehta, A.D., Mégevand, P., Groppe, D.M., and Zion-Golumbic, E. (2017). Low-frequency cortical oscillations entrain to subthreshold rhythmic auditory stimuli. J. Neurosci. *37*, 4903–4912.

Park, H., Lee, D.S., Kang, E., Kang, H., Hahm, J., Kim, J.S., Chung, C.K., Jiang, H., Gross, J., and Jensen, O. (2016). Formation of visual memories controlled by gamma power phase-locked to alpha oscillations. Sci. Rep. *6*, 28092.

Pegado, F., Vankrunkelsven, H., Steyaert, J., Boets, B., De Beeck, H.O., and Op de Beeck, H. (2016). Exploring the Use of Sensorial LTP/LTD-Like Stimulation to Modulate Human Performance for Complex Visual Stimuli. PNAS *11*, e0158312.

Pelli, D.G. (1997). The VideoToolbox software for visual psychophysics: transforming numbers into movies. Spat. Vis. *10*, 437–442.

Poggio, T., Fahle, M., Edelman, S., Askenasy, J., Sagi, D., Science, S.E.-, and 1992, undefined (1992). Fast perceptual learning in visual hyperacuity. Science (80-.). *256*, 1018–1021.

Porciatti, V., Pizzorusso, T., and Maffei, L. (1999). The visual physiology of the wild type mouse determined with pattern VEPs. Vision Res. *39*, 3071–3081.

Saleem, A.B., Lien, A.D., Krumin, M., Haider, B., Rosón, M.R., Ayaz, A., Reinhold, K., Busse, L., Carandini, M., Harris, K.D., et al. (2017). Subcortical Source and Modulation of the Narrowband Gamma Oscillation in Mouse Visual Cortex. Neuron *93*, 315–322.

Sanders, P.J., Thompson, B., Corballis, P.M., Maslin, M., and Searchfield, G.D. (2018). A review of plasticity induced by auditory and visual tetanic stimulation in humans. Eur. J. Neurosci. *48*, 2084–2097.

Sauseng, P., Klimesch, W., Gruber, W.R.R., Hanslmayr, S., Freunberger, R., and Doppelmayr, M. (2007). Are event-related potential components generated by phase resetting of brain oscillations? A critical discussion (Pergamon).

Sohal, V.S., Zhang, F., Yizhar, O., and Deisseroth, K. (2009). Parvalbumin neurons and gamma rhythms enhance cortical circuit performance. Nature *459*, 698–702.

Spaak, E., Bonnefond, M., Maier, A., Leopold, D.A., and Jensen, O. (2012). Layer-Specific Entrainment of Gamma-Band Neural Activity by the Alpha Rhythm in Monkey Visual Cortex. Curr. Biol. *22*, 2313–2318.

Stark, E., Eichler, R., Roux, L., Fujisawa, S., Rotstein, H.G., and Buzsáki, G. (2013). Inhibition-Induced theta resonance in cortical circuits. Neuron *80*, 1263–1276.

Stringer, C., Pachitariu, M., Steinmetz, N., Reddy, C.B., Carandini, M., and Harris, K.D. (2019). Spontaneous behaviors drive multidimensional, brainwide activity. Science *364*, 255.

Tanimoto, N., Sothilingam, V., Kondo, M., Biel, M., Humphries, P., and Seeliger, M.W. (2015). Electroretinographic assessment of rod- and cone-mediated bipolar cell pathways using flicker stimuli in mice. Sci. Rep. *5*, 10731.

Veit, J., Hakim, R., Jadi, M.P., Sejnowski, T.J., and Adesnik, H. (2017). Cortical gamma band synchronization through somatostatin interneurons. Nat. Neurosci. *20*, 951–959.

Whitlock, J.R., Heynen, A.J., Shuler, M.G., and Bear, M.F. (2006). Learning induces long-term potentiation in the hippocampus. Science (80-.). *313*, 1093–1097.

Williams, J.. (2001). Frequency-specific effects of flicker on recognition memory. Neuroscience *104*, 283–286.

Williams, J., Ramaswamy, D., and Oulhaj, A. (2006). 10 Hz flicker improves recognition memory in older people. BMC Neurosci. *7*, 21.

Xing, D., Yeh, C.I., Burns, S., and Shapley, R.M. (2012). Laminar analysis of visually evoked activity in the primary visual cortex. Proc. Natl. Acad. Sci. U. S. A. *109*, 13871–13876.

Xu, D., Hopf, C., Reddy, R., Cho, R.W., Guo, L., Lanahan, A., Petralia, R.S., Wenthold, R.J., O'Brien, R.J., and Worley, P. (2003). Narp and NP1 Form Heterocomplexes that Function in Developmental and Activity-Dependent Synaptic Plasticity. Neuron *39*, 513–528.

Yao, H., Shi, L., Han, F., Gao, H., and Dan, Y. (2007). Rapid learning in cortical coding of visual scenes. Nat. Neurosci. *10*, 772–778.

Zaehle, T., Clapp, W.C., Hamm, J.P., Meyer, M., and Kirk, I.J. (2007). Induction of LTP-like changes in human auditory cortex by rapid auditory stimulation: An FMRI study. Restor. Neurol. Neurosci. *25*, 251–259.

Zold, C.L., and Hussain Shuler, M.G. (2015). Theta Oscillations in Visual Cortex Emerge with Experience to Convey Expected Reward Time and Experienced Reward Rate. J. Neurosci. *35*, 9603–9614.

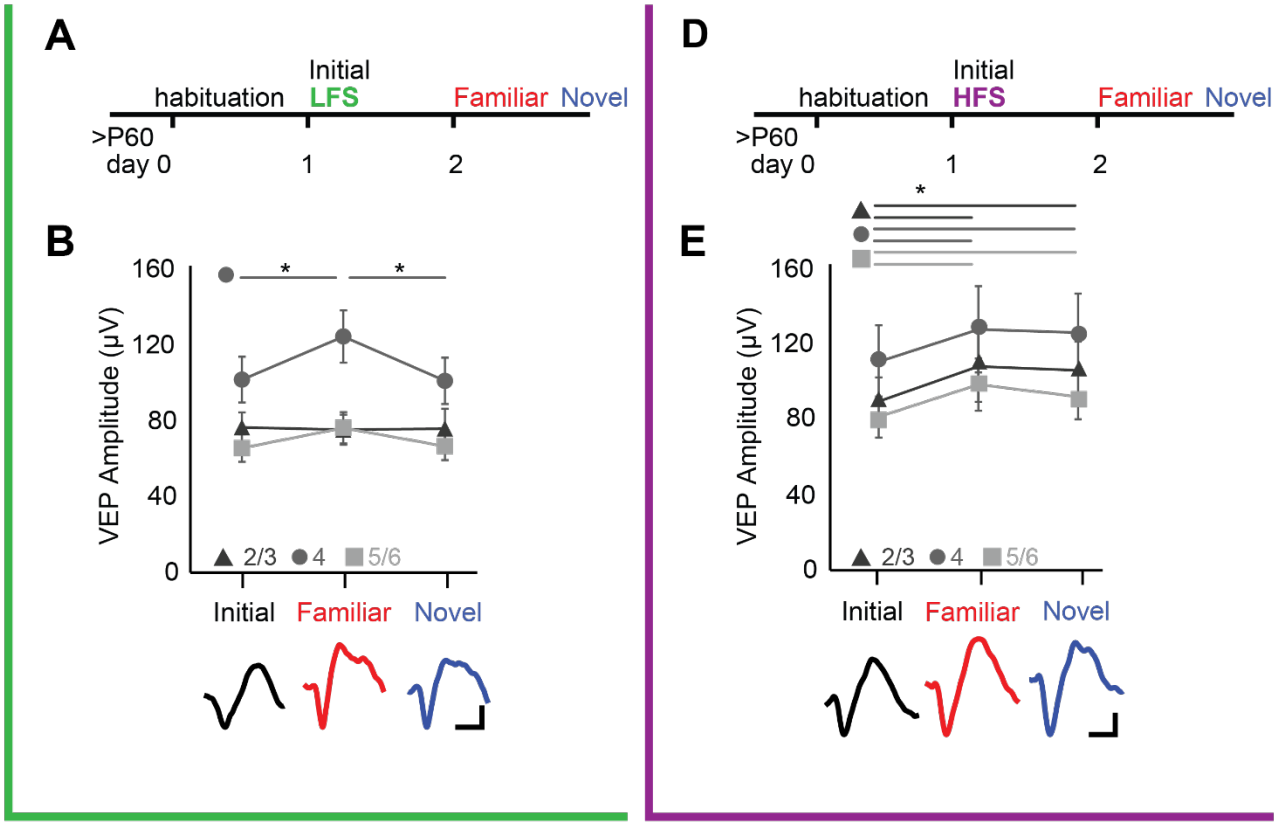

Figure 1.

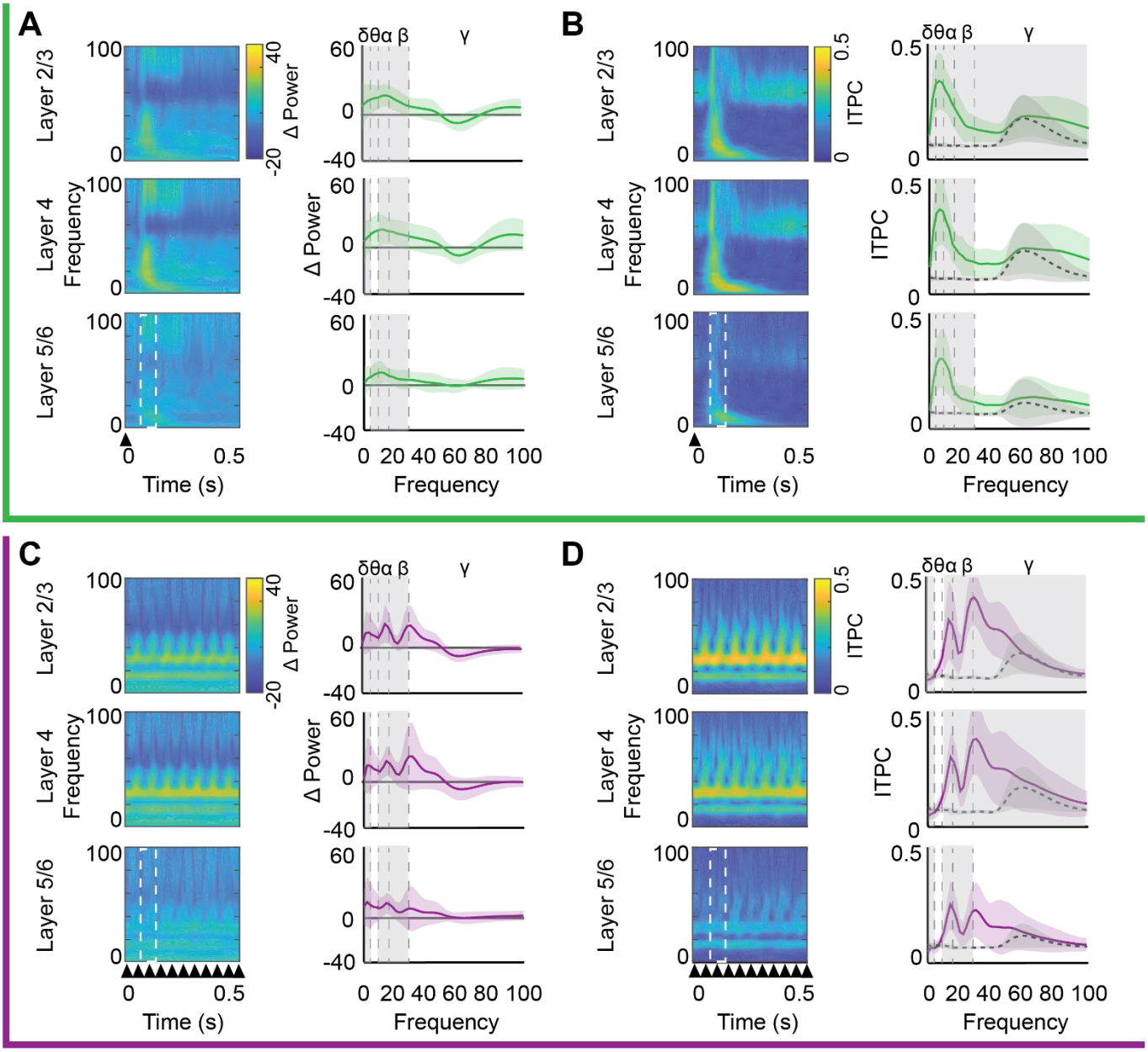

Figure 2.

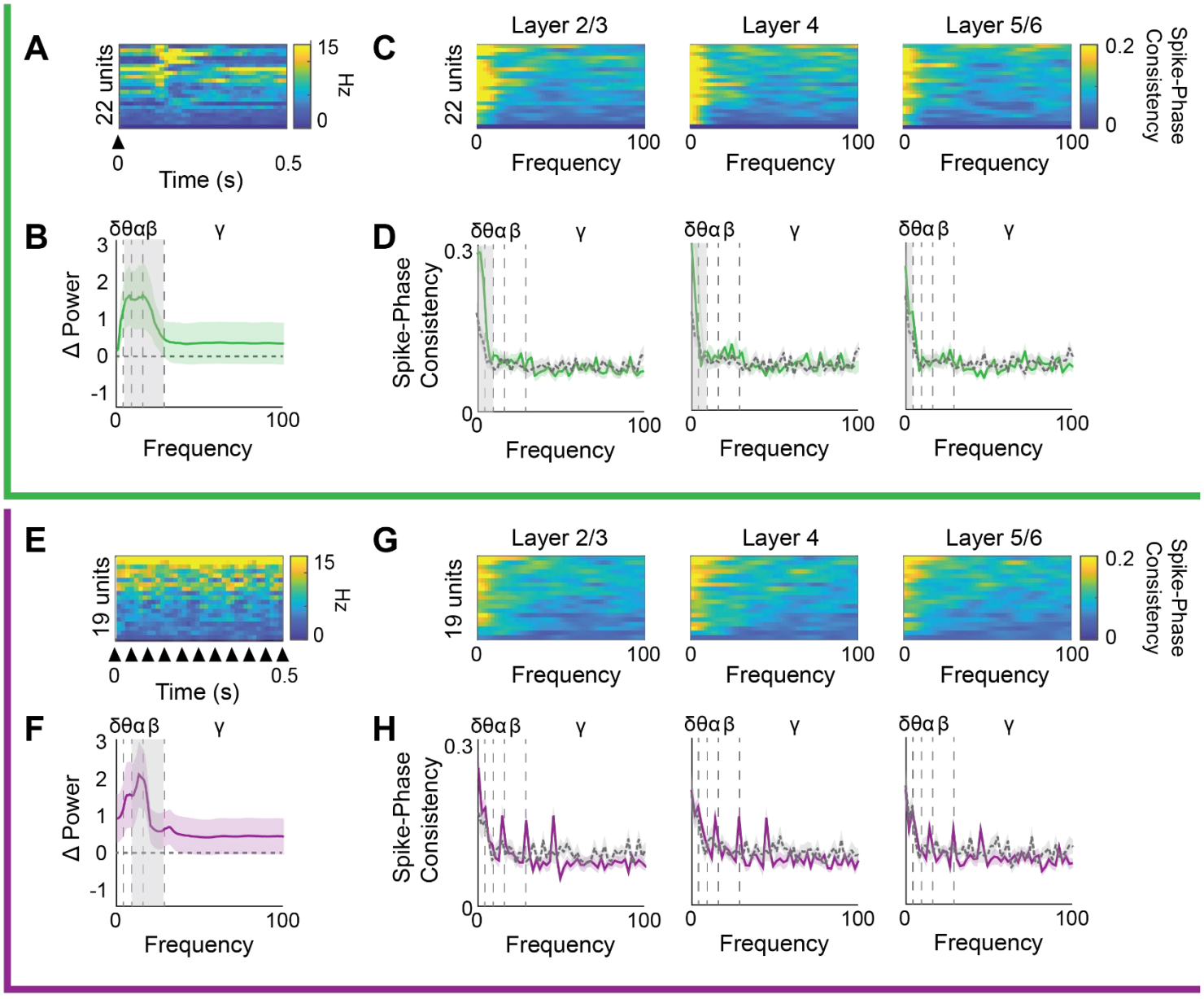

Figure 3.

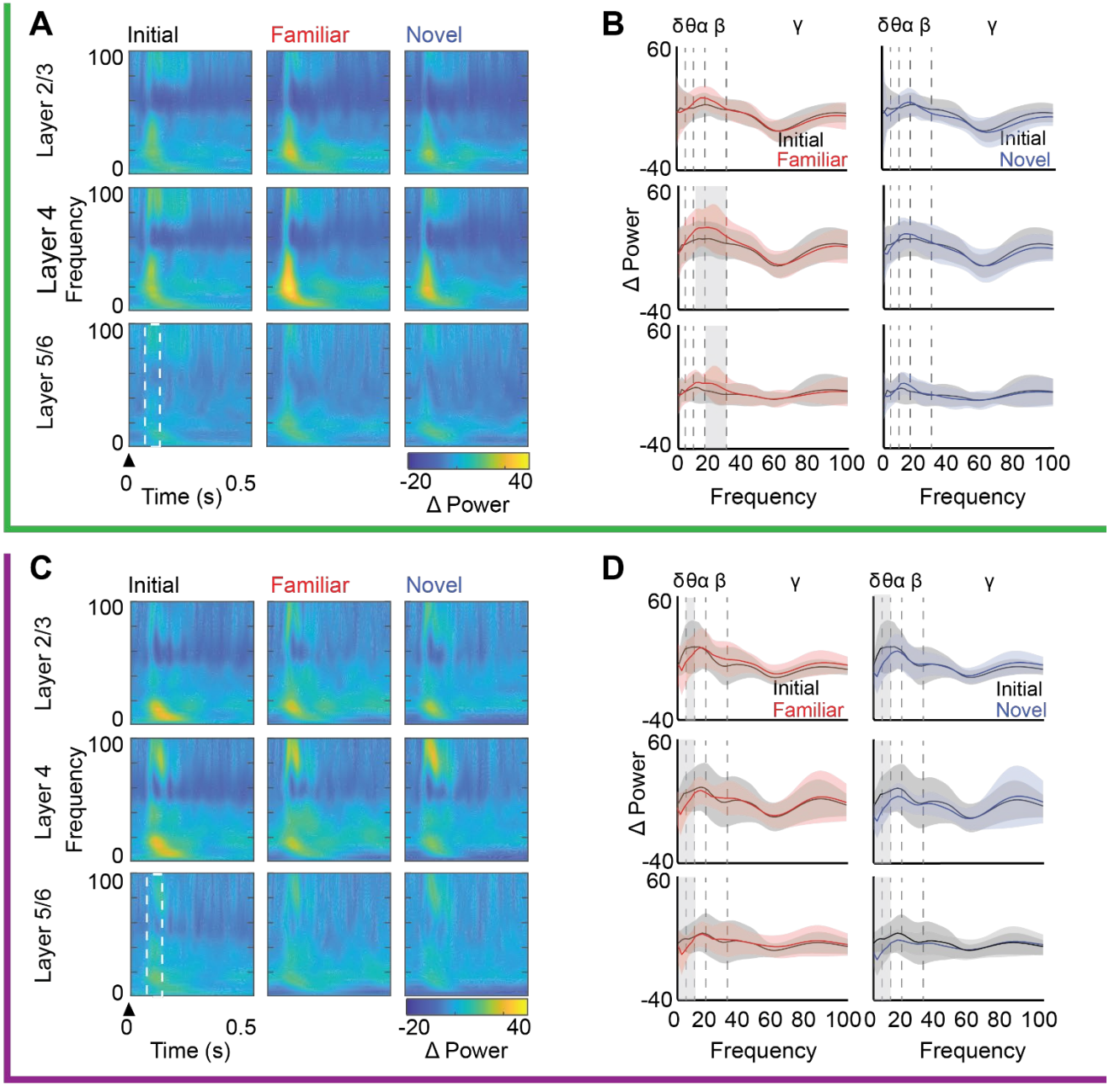

Figure 4.

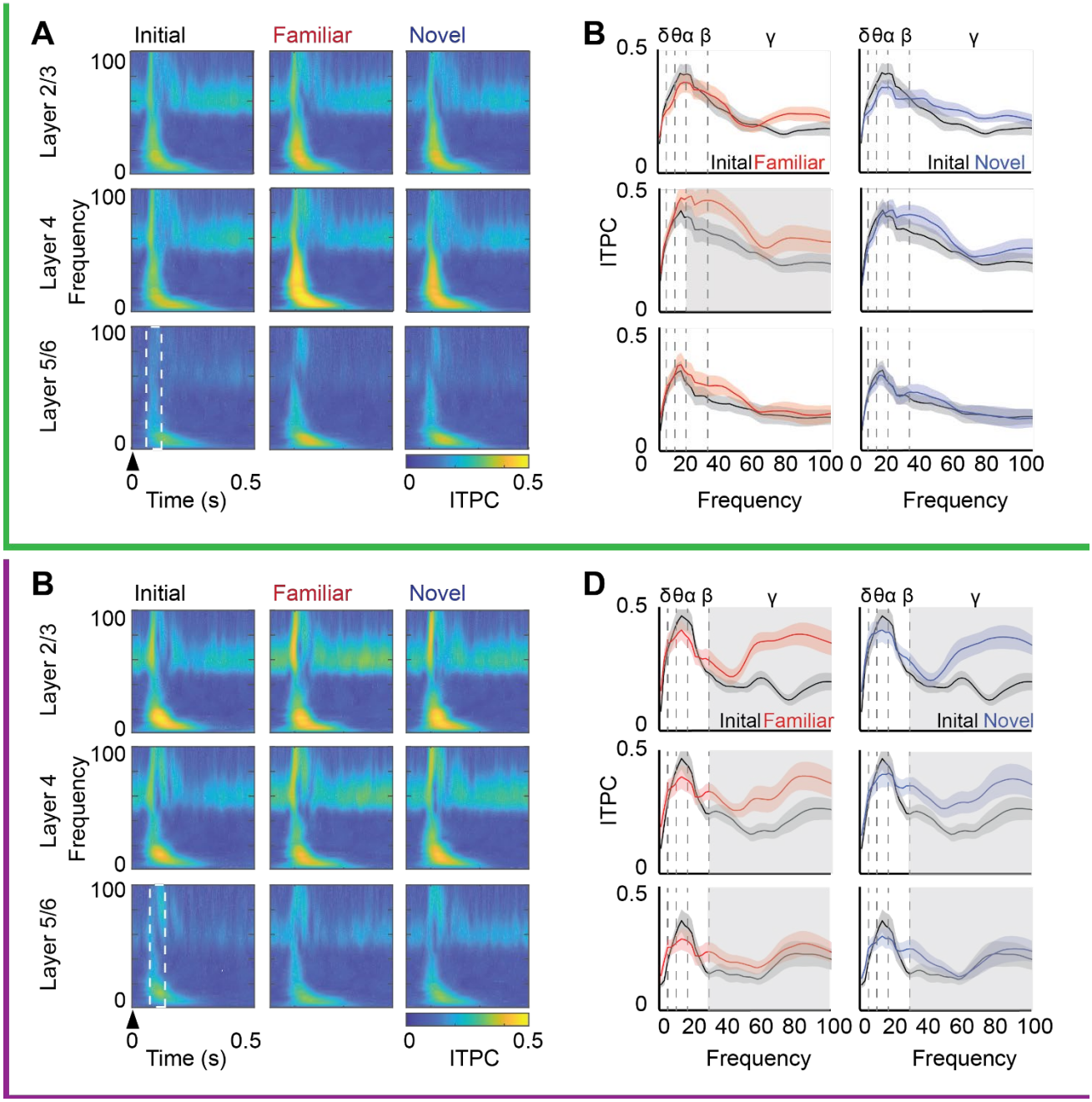

Figure 5.

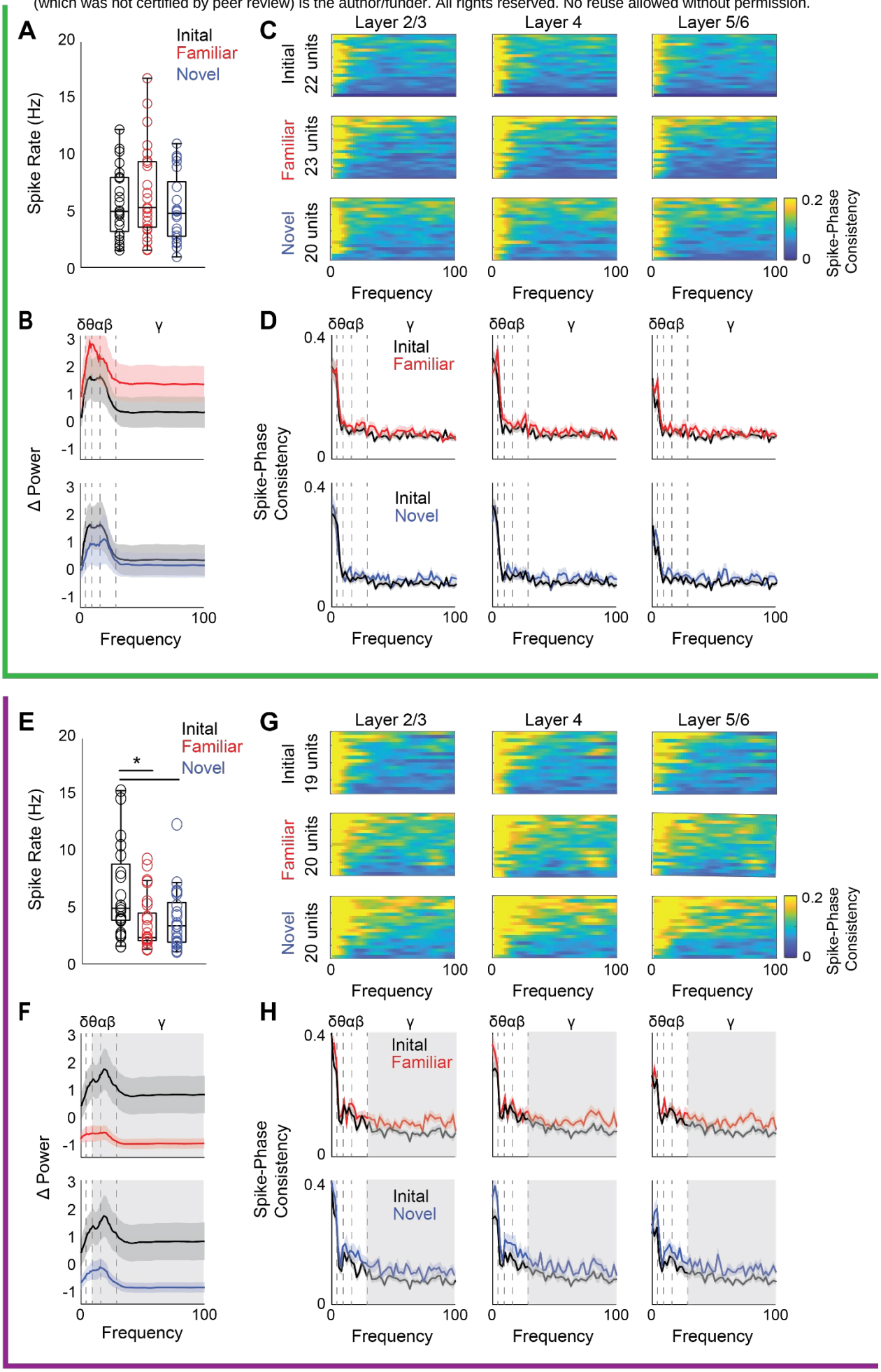

Figure 6.

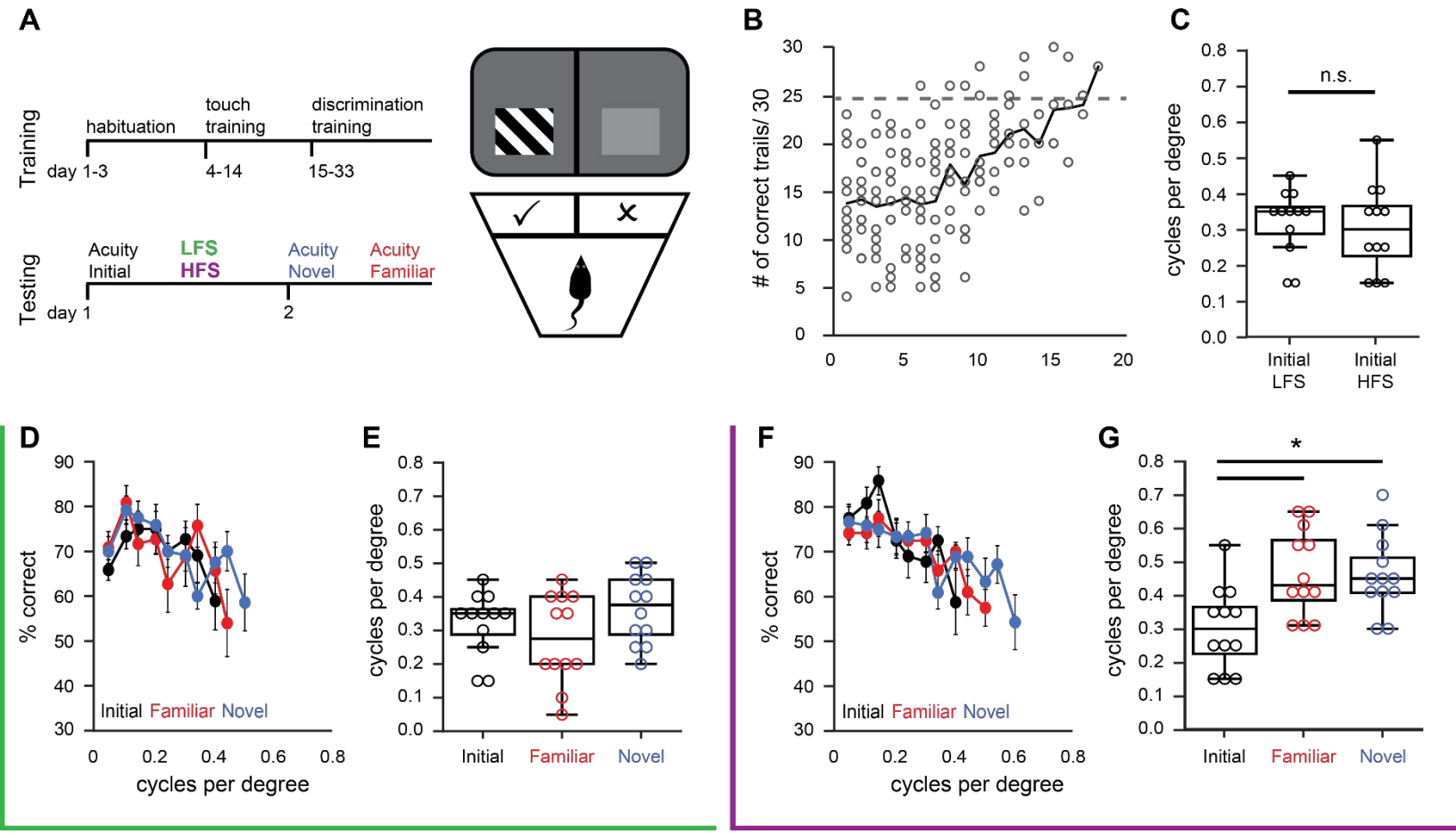

Figure 7.

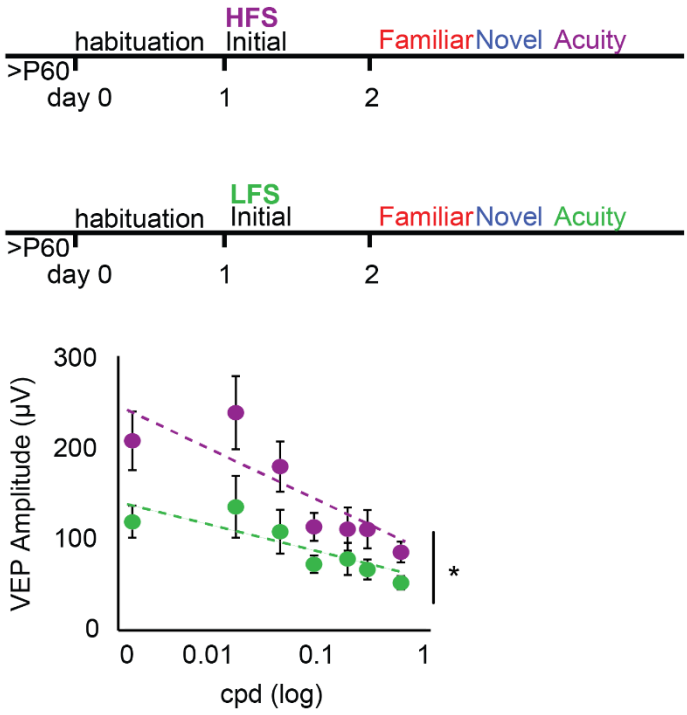

Figure S1.

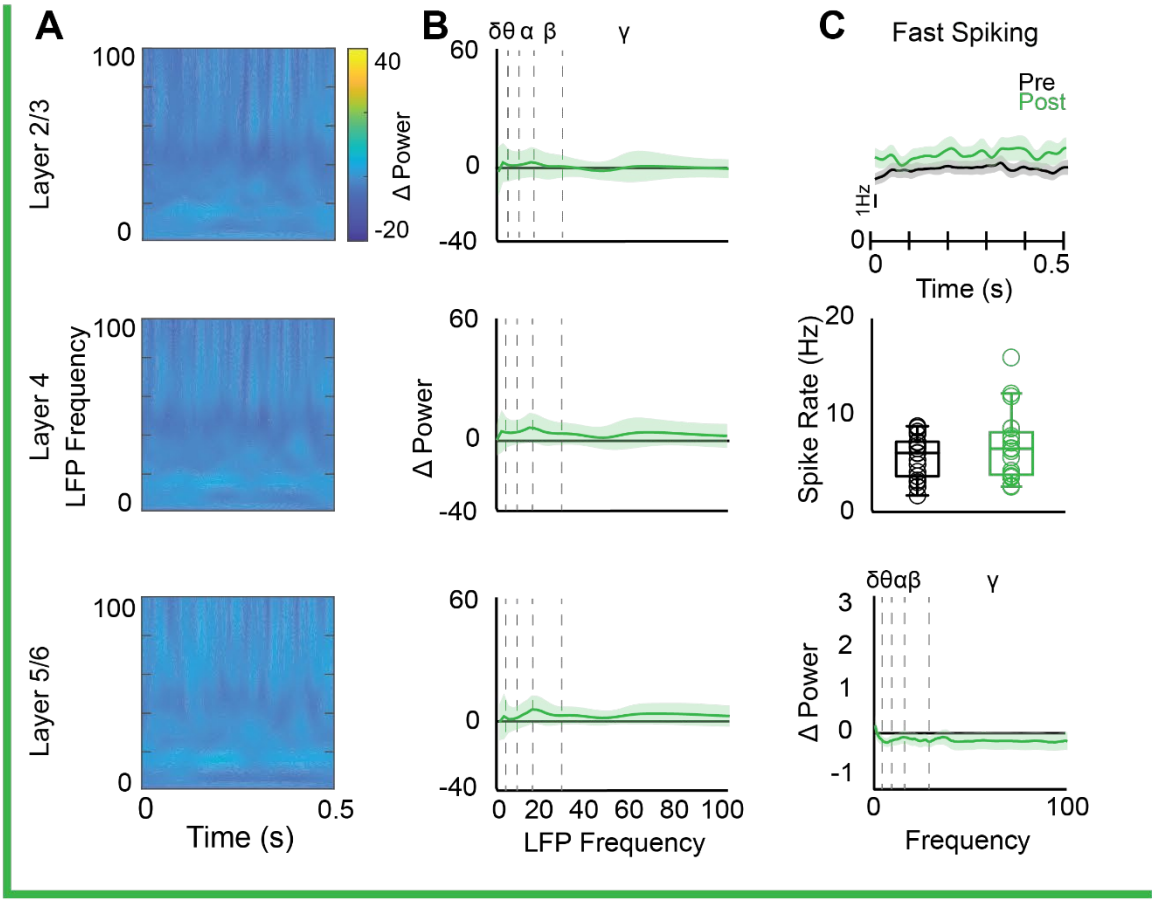

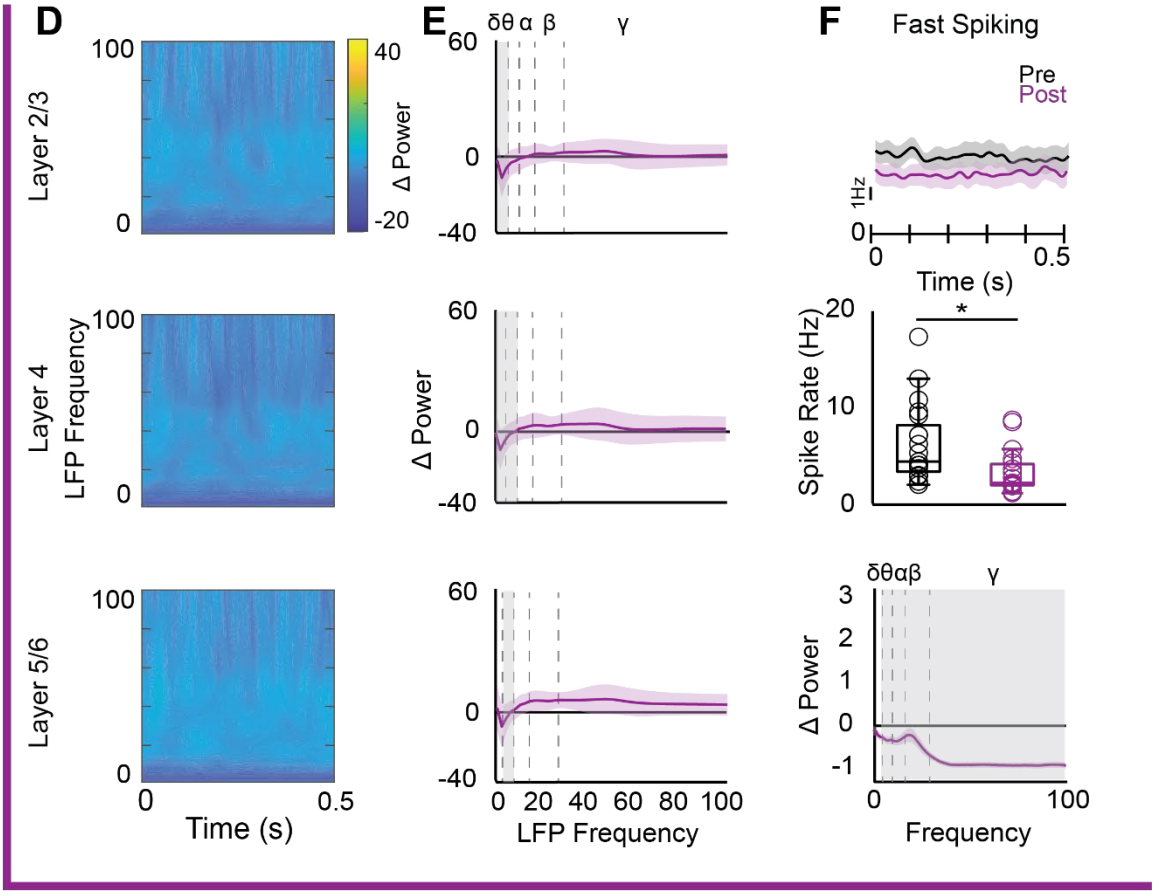

Figure S2.